University of Alberta
Department of Civil Engineering

Structural Engineering Report No. 26

Buckling Strength of Hot Rolled Hat Shaped Sections

by

D. A. Heaton

and

P. F. Adams

July, 1970

BUCKLING STRENGTH OF HOT ROLLED HAT SHAPED SECTIONS

BY

D.A. HEATON

P.F. ADAMS

JULY, 1970

DEPARTMENT OF CIVIL ENGINEERING

UNIVERSITY OF ALBERTA

EDMONTON, CANADA

ABSTRACT

Hot rolled hat shaped sections are commonly used as chord members in open web steel joists. It is normally assumed that the ultimate strength of the compression chord is given by its flexural buckling strength. However, as the hat shaped sections have only one axis of symmetry, buckling can occur in either a flexural, or a lateral torsional mode. In this investigation, the flexural and lateral torsional buckling strengths of hot rolled hat shaped sections were investigated over a wide range of slenderness ratios.

Residual strain and yield stress distributions were determined for the member and a uniform axial strain applied. Section properties of the elastic core and the load corresponding to the applied strain level were evaluated. The differential equations expressing equilibrium of the member in the deformed shape were entered with this load and the appropriate section properties, and the critical lengths corresponding to flexural and lateral torsional buckling were computed. This procedure was repeated for different values of the applied strain until the complete column curve for the member had been determined.

The effects of different yield stress distributions on the buckling strength were examined. However, even with the most severe distribution, lateral-torsional buckling was not critical. A comparison was made between the critical buckling stresses and those permitted by the allowable stress sections of C.S.A. S16 1969. These provisions result in adequate factors of safety.

TABLE OF CONTENTS

CHAPTER I

INTRODUCTION

Open web steel joists are widely used as simply supported flexural members to support roofs and lightly loaded floors. A typical joist is shown in FIG. 1.1. The arrangement of the web members permits easy passage of heating ducts and other services through the joist. Joists also offer savings in weight over comparable members having solid webs.

Various sections are used for the chord members of open web steel joists. These include circular bars, tees and double angles. However, perhaps the most popular chord member is the hat-shaped section. A typical hat-shaped section is shown in FIG. 1.2. In this figure the principal axes, designated x and y, are shown passing through the centroid, C. The section is symmetrical about the y axis and the shear centre, S, is located on the y axis, a distance y_0 below the centroid.

Hat shaped sections have normally been fabricated from light gauge steel strip by a cold forming process.(1) However, more recently, much heavier hat shaped sections have been produced by hot rolling.

The forces acting on a typical compression chord segment of length, L, are shown in FIG. 1.3. The chord is subjected to a transverse load, w, which may be concentrated or uniformly distributed, depending on how the floor or roof system bears on the chord. As the joist is loaded, bending moments M_1 and M_2 are induced in the chord as well as shears, V_1 and V_2, and axial compressive forces P_1 and P_2. The web members develop primarily axial forces, F_1, F_2, F_3 and F_4. The transverse load, bending moment, and accompanying shears are usually small and it is assumed that the primary force is the axial thrust induced by the truss action of the joist.

Due to the close spacing between web-chord connections, or panel points, the axial loads in adjacent chord segments will vary only slightly. Thus, when a critically loaded segment of the chord is on the verge of buckling between panel points, the adjacent chord segments are also near failure and can offer little restraint to the critical segment. Hence each chord segment may be assumed to be pin connected. The simplified chord segment model is shown in FIG. 1.3b.

The idealized chord segment is subjected to an axial thrust and if premature local buckling does not occur, the ultimate strength of the segment is conservatively predicted by the buckling strength.(2,3) The buckling strength can be shown schematically on a "column curve". FIGURE 1.4 is a typical column curve which relates the slenderness ratio, KL/r, to the average applied stress at the instant of buckling, σ. The buckling stress is non-dimensionalized as σ/σ_y, where σ_y is the yield stress of the material. The effective length is represented by KL and r denotes the radius of gyration of the cross section.

The dashed line in FIG. 1.4 represents the behavior of a member composed of an elastic material. The behaviour of very slender steel columns is predicted by this curve. These slender columns buckle with the complete cross section subjected to strains within the elastic range. A column composed of an elastic perfectly plastic material deviates abruptly from the elastic curve when the applied axial stress equals the yield stress.

Structural steel members contain residual strains and, in addition, may have variations in yield stress over the cross section. These properties cause premature yielding in parts of the cross section at an average applied stress considerably below the yield stress. The local yielding causes the member behavior to deviate from that depicted by the elastic curve as buckling of the member occurs after portions of the cross section have yielded. This is termed inelastic buckling.

Monosymmetric sections can buckle in either a pure flexural mode or a lateral torsional mode.[4] The two possible positions are shown in FIG. 1.5. A flexural buckling motion is resisted by the bending strength of the member while lateral torsional buckling involves both the flexural and torsional resistances of the member.

In the absence of more complete information, hat shaped sections have been designed on the basis of their flexural buckling strengths. The purpose of this investigation is to compute the flexural and lateral-torsional buckling strengths for a variety of hot rolled shaped members commonly used in open web steel joists. The variations in material properties and residual strains will be examined and their effects incorporated into the analysis. For the purposes of this investigation, the model of the joist segment is considered to be that shown in FIG. 1.3b.

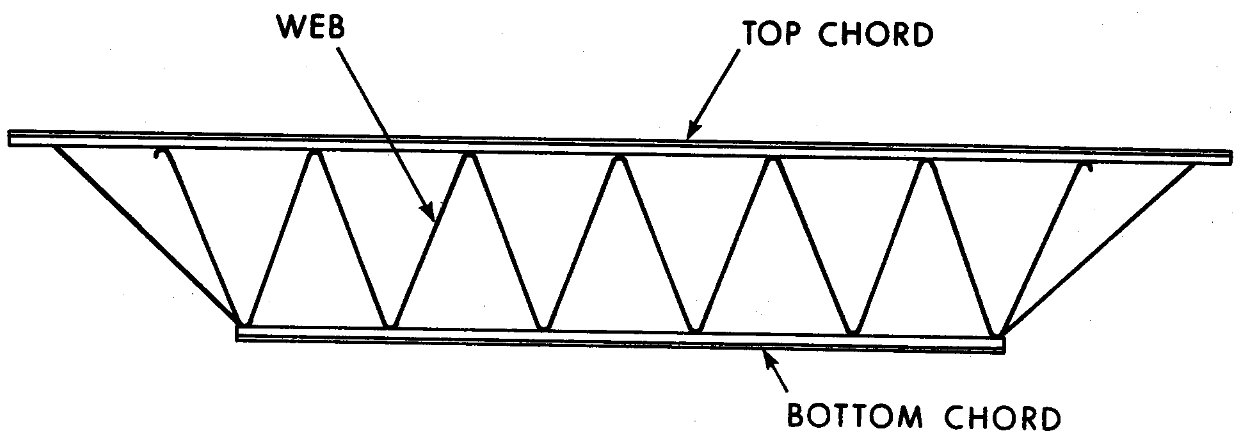

FIG. 1.1 TYPICAL OPEN WEB STEEL JOIST

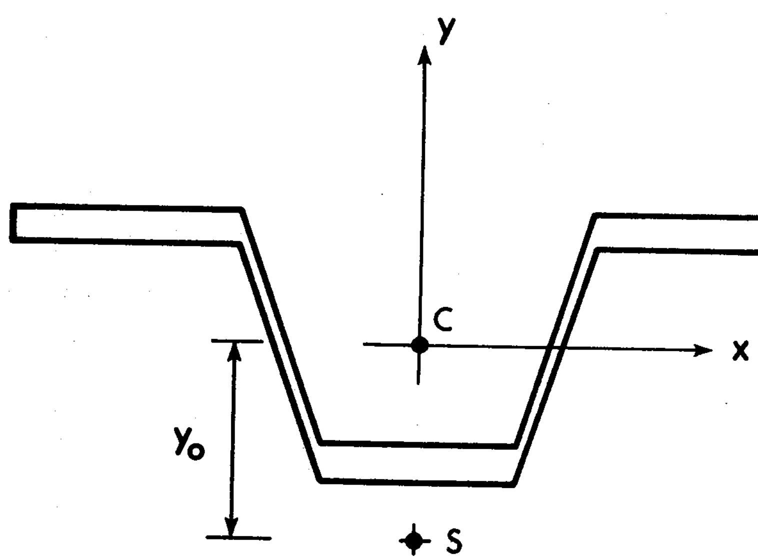

FIG. 1.2 TYPICAL HAT SHAPED SECTION

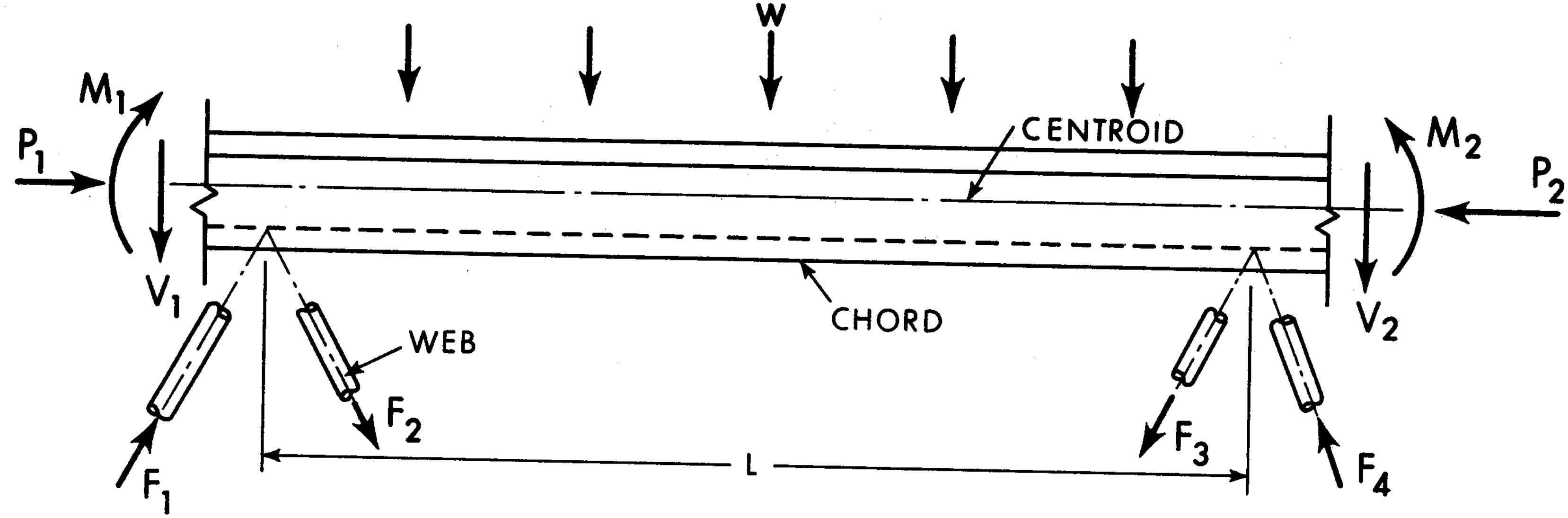

CHORD SEGMENT

FIG. 1.3a CHORD SEGMENT

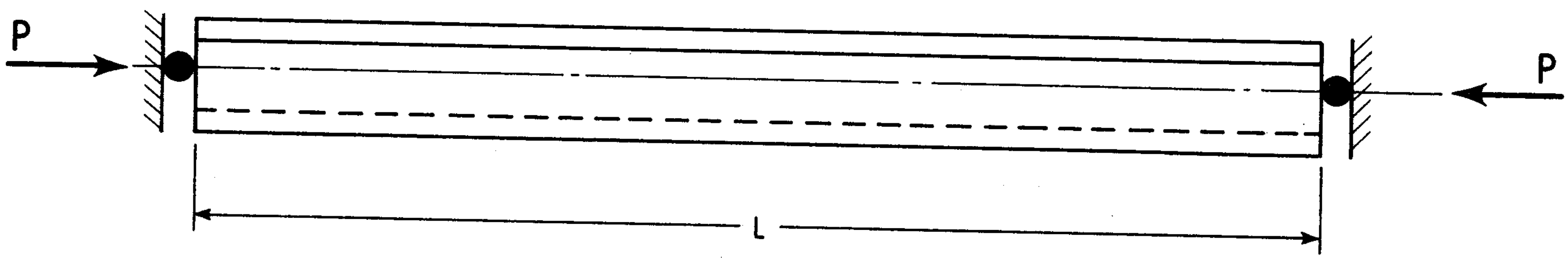

SIMPLIFIED CHORD SEGMENT

FIG. 1.3b SIMPLIFIED CHORD SEGMENT

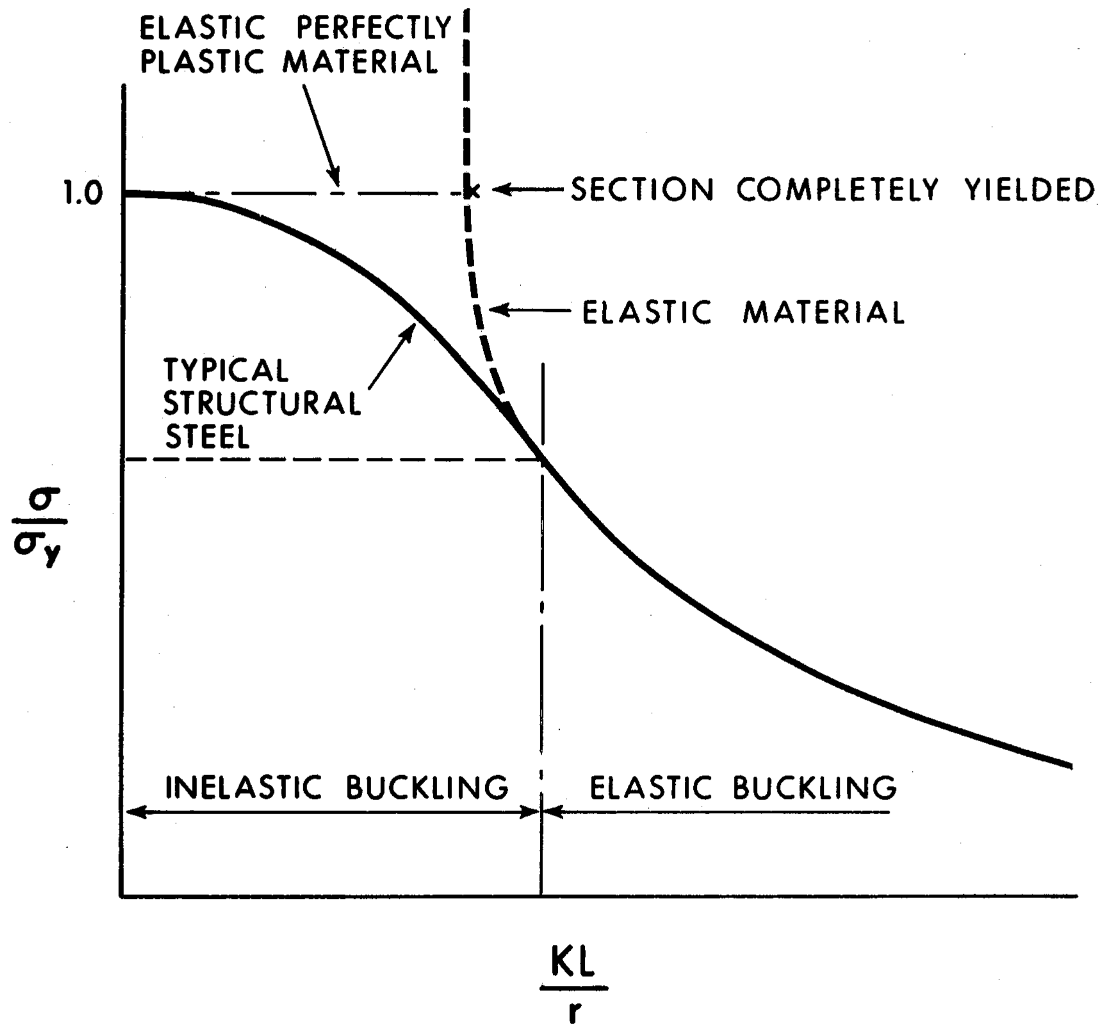

FIG. 1.4 COLUMN CURVE

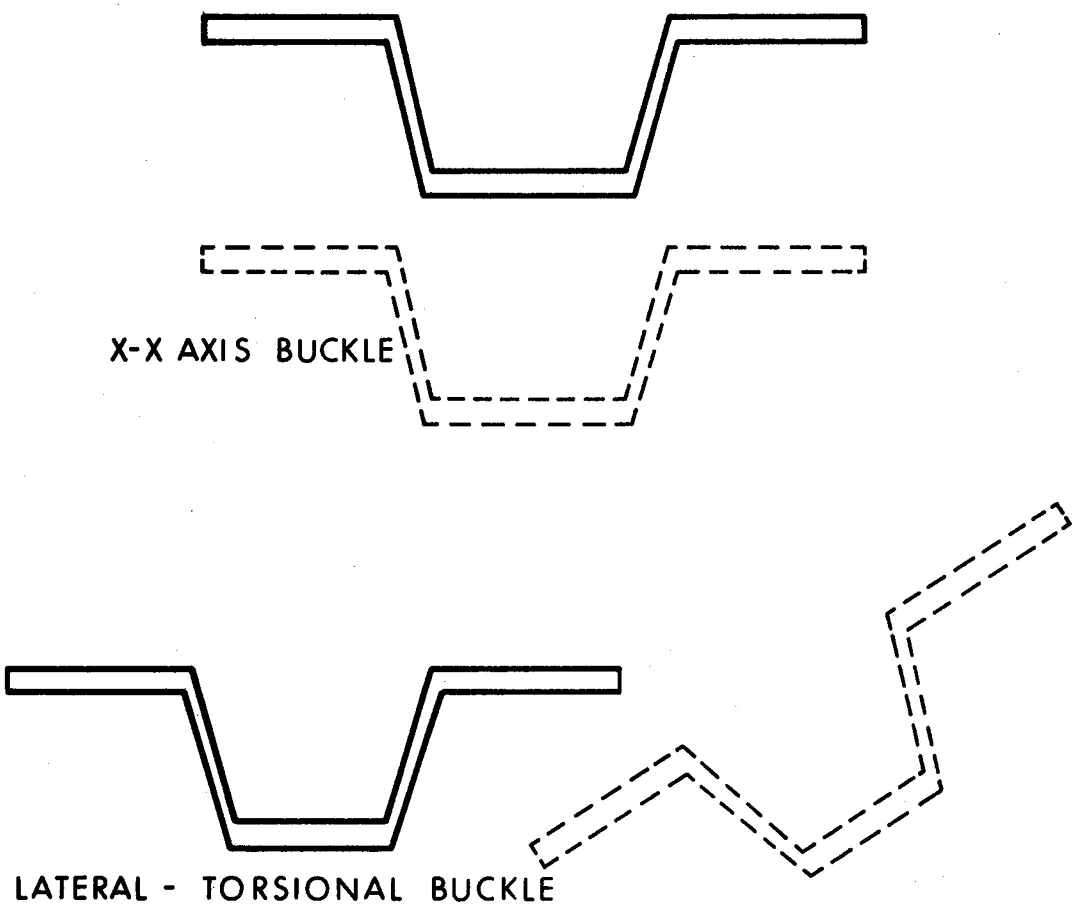

FIG. 1.5 BUCKLING MODES OF HAT SHAPED SECTIONS

CHAPTER II

PREVIOUS INVESTIGATIONS

The equations expressing the equilibrium of a monosymmetric column section in the deformed position are given below[5]

$$EI_x v'''' + Pv'' = 0 \tag{2.1}$$

$$EI_y u'''' + Pu'' + Py_o \phi'' = 0 \tag{2.2}$$

$$EI_w \phi'''' - (GK_T + \overline{K})\phi'' + Py_o u'' = 0 \tag{2.3}$$

FIGURE 2.1 shows the column and the deformed positions of the cross section.

In the above equations, E represents the modulus of elasticity, G, the torsional modulus of the material and P, the axial load. I_x and I_y denote the moments of inertia about the x and y axes respectively. The distance between the centroid and the shear centre is represented by y_o. K_T denotes the St. Venant torsional stiffness while I_w represents the warping moment of inertia of the cross section. $\overline{K} = \int_A \sigma a^2 dA$ where A is the area of the cross section, σ the total stress on the fibre and a is the distance from the fibre to the shear centre. The quantities, u, v and ϕ represent displacements of the shear centre as shown in FIG. 2.1, and the primed quantities denote differentiation with respect to z.

For simply supported flexural and torsional boundary conditions, the solutions to the equations take the form:

$$v = C_1 \sin \frac{\pi Z}{L} \qquad 2.4$$

$$u = C_2 \sin \frac{\pi Z}{L} \qquad 2.5$$

$$\phi = C_3 \sin \frac{\pi Z}{L} \qquad 2.6$$

Substituting for the deflections and their derivatives into equations 2.1, 2.2 and 2.3 results in three homogeneous linear equations in terms of the constants C_1, C_2 and C_3. The equation resulting from Eqn. 2.1 is independent of the other two, and its solution is the critical load for flexural buckling about the x-axis;

$$(P_x)_{cr} = \pi^2 EI_x/L^2 \qquad 2.7$$

The equations resulting from Eqns. 2.2 and 2.3 are coupled and combine to give a quadratic solution for the critical lateral torsional buckling load, $(P_{yT})_{cr}$.

$$(P_y - (P_{yT})_{cr})(P_z + \overline{K}) - (P_{yT})^2{}_{cr}\, y_o{}^2 = 0 \qquad 2.8$$

where

$$P_y = \pi^2 EI_y/L^2 \qquad 2.9$$

and

$$P_z = \pi^2 EI_w/L^2 + GK_T \qquad 2.10$$

If the section properties of the member are known, the solution of equations 2.7 and 2.8 is routine and the lower critical load represents the buckling strength. However, for members of practical proportions, portions of the cross-section yield before buckling occurs due to variations in yield stress and the presence of residual strains. This partial yielding means that the elastic buckling equations no longer apply directly, since the section properties of the elastic core change as shown in FIG. 2.2.

The buckling strength of the member is therefore profoundly affected by the residual strain distribution and by the variations in yield stress across the section.

For WF shapes the standard technique used to determine the residual strain distribution is to remove a selected length from the member. Longitudinal strips are then marked on this section, and the residual strain in each strip is determined by noting the change in length of the strip after it is cut from the section. The measurements are performed on both sides of each strip using a Whitemore Strain Gauge. This method could not be used for tubular members as only one side of the strips was accessible prior to cutting(6). An alternative method, devised for these members, was to measure the change in length and the change in curvature on one side of the strip only, when the strips were cut free. During the course of this investigation, the subsequent bowing of the strips when cut free influenced the apparent residual strain[6]. The bowing action was accounted for in the curvature measurements so the computed residual strains were correct.

The effect of bowing is shown in FIG. 2.3. Corrections for the bowing action should still be applied even where changes in length are measured on both sides of the strip. The change in mid-thickness length, due to residual strains, should be computed as the difference between the original lengths, OL_1, OL_2, and final arc lengths AL_1, AL_2. In the presence of significant bowing, the standard method computes the change in length inaccurately as the differences between the original lengths and the chord lengths CL_1, CL_2. These differences measured for both sides are averaged to obtain the change in mid-thickness length. This process only removes the error due to the offset, e, of the points of the Whitemore Strain Gauge from the centreline of the gauge holes.

The tangent modulus approach to buckling assumes yielded portions of the cross section to be ineffective in resisting the buckling motion. This approach also makes no allowance for the increase in strength caused by the elastic unloading of previously yielded fibres. The concept is conservative, and is recommended as a basis for design by the Column Research Council[7]. It is implied in this concept that only the elastic core of the cross section is effective in resisting the buckling motion.

Buckling strength of WF shapes, using the tangent modulus approach have been established for many different cross sections, materials, and residual strain distributions.[8] In assessing the torsional buckling strengths[8], it has been assumed that the residual stress distribution must satisfy the relationship

$$\int_A \sigma_r \cdot a^2 \, dA = 0 \qquad 2.11$$

where σ_r denotes the residual stress on a fibre. Thus $\overline{K}$ is given by:

$$\overline{K} = - P({x_o}^2 + {y_o}^2 + \frac{I_x + I_y}{A}) \qquad 2.12$$

However, since both the shearing and normal residual stresses on any section can be in equilibrium without satisfying equation 2.11, the relationship is not a necessary one.[8]

Buckling strengths for cold rolled hat shaped sections,[13] have been established in the elastic range ignoring the effects of residual strains.[9] This study was extended to allow for eccentric loads and inelastic action but residual strain effects were again neglected.[10] Cold rolled sections have such a large variation in yield stress across the section that residual strain effects are masked. The magnitude of this variation can be seen in FIG. 2.4. This variation in yield stress was accounted for in an investigation into the flexural buckling strength of cold rolled hat shaped sections.[1]

An indirect approach to the determination of the tangent modulus for hot shaped column sections has also been described in the literature.[11] The complete flexural buckling curve was determined by using the results of stub column tests to establish an effective bending stiffness.

The present investigation is aimed at evaluating the flexural and lateral-torsional buckling strengths of hot rolled hat shaped column sections. The effects of the residual strains and yield stress variation will be accounted for and the investigation will cover the complete practical range of column slenderness.

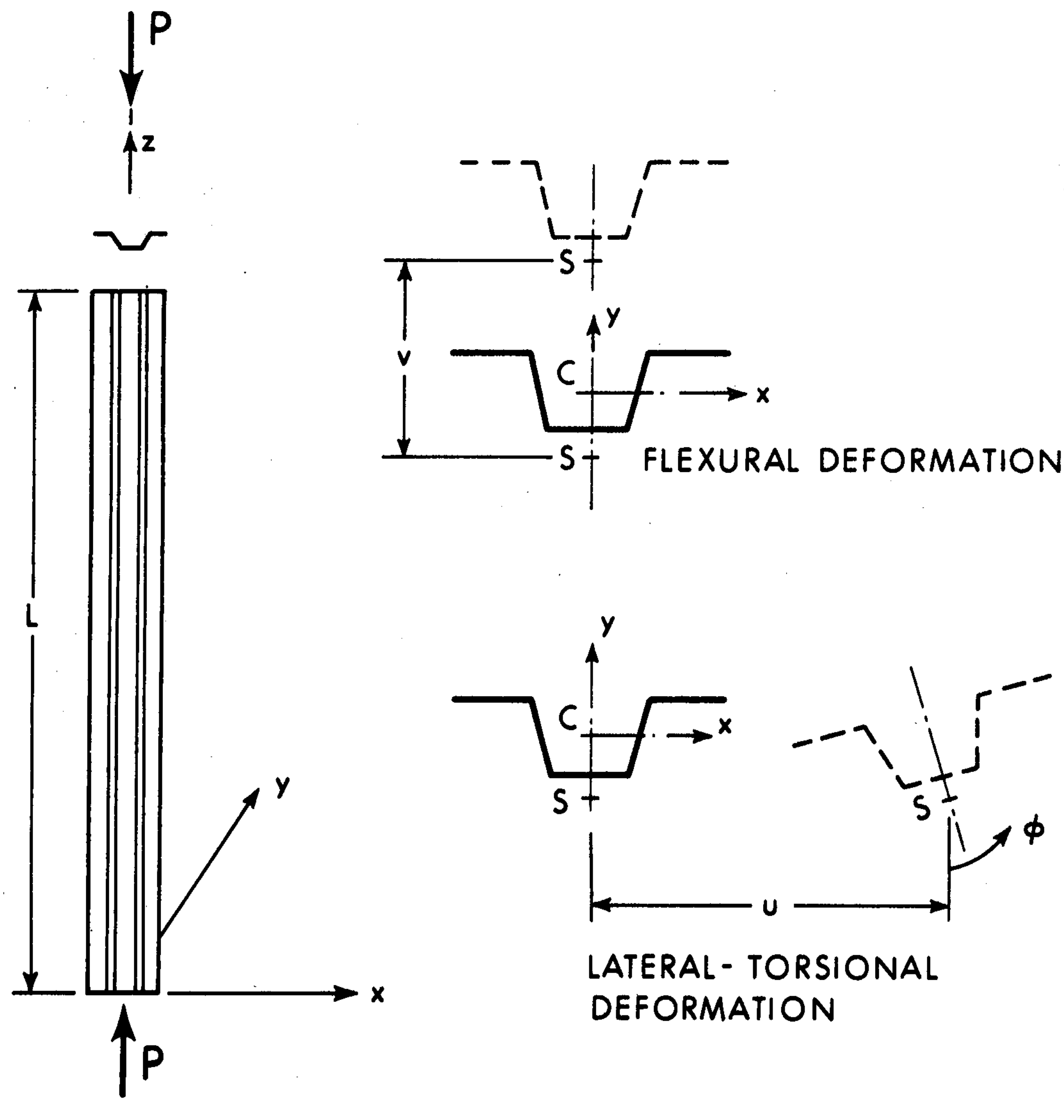

FIG. 2.1 NOMENCLATURE USED IN THE DIFFERENTIAL EQUATIONS OF BUCKLING

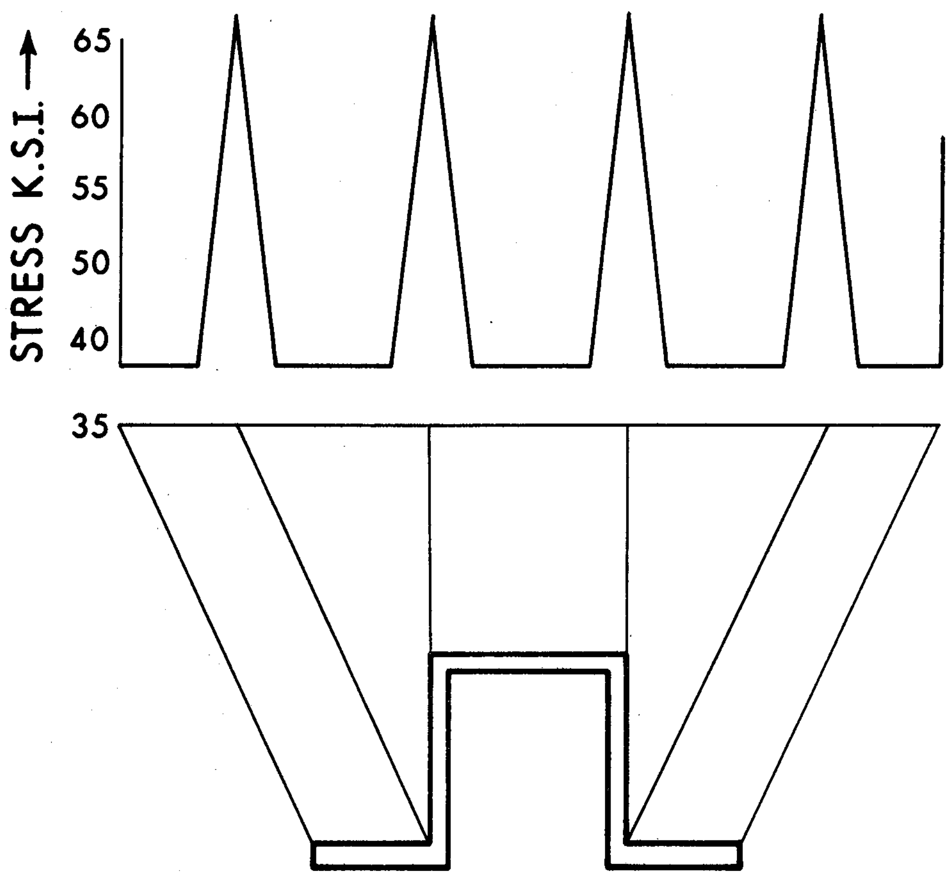

FIG. 2.4 VARIATIONS IN YIELD STRESS - COLD FORMED HAT SHAPED SECTIONS

CHAPTER III

MATERIAL AND SECTION PROPERTIES

The steel used in the chords is produced especially for the manufacturer of the open web joists and is not covered by a C.S.A. specification. However, a specified chemical composition as well as a minimum yield stress of 55 k.s.i. are required. A typical chemical analysis for this steel is shown in Table 3.3. Tension coupons cut from the web of the hat section are used in the mill tests to determine the yield stress.

The complete range of hot rolled hat shaped sections which were available for this investigation is shown in FIG. 3.1. Sections were chosen from this group which should exhibit the most severe distribution of residual strains as well as significant variations in yield stress over the cross section.

The residual strain distribution is produced by differential cooling and plastic flow of the cross section during its manufacture. The pattern of differential cooling is affected primarily by the length and thickness of the flanges. Sections E, F and L, shown in FIG. 3.3, were chosen to investigate the possible different residual strain distributions. The difference in the residual strain results obtained from E and F should be caused primarily by the difference in flange length while the difference in results between sections F and L would be caused by the variation in flange thickness.

The yield stress is affected by the differences in the grain structures of the steel produced by different rates of cooling. Section L was accordingly chosen to investigate variations in yield stress as portions of this section should have experienced the widest variation in cooling rates compared to other sections. Dimensions of section L are given in FIG. 3.2.

Table 3.1 lists the material properties obtained from tension tests on specimens cut from section L. A length of this section was cut into eight strips as shown in FIG. 3.2. The strips were then machined to tension coupons and tested in a hydraulic testing machine. The static yield stress, σ_y, was obtained by holding the specimen at a constant strain for five minutes. A modulus of elasticity, E, equal to 29,600 kips/ins^2 was used to compute the yield strain, ε_y, as σ_y/E. The strain hardening modulus, E_{st}, was taken as the slope of the tangent to the initial part of the strain hardening portion of the curve. The strain at the onset of strain hardening is denoted by ε_{st} and the ultimate stress as σ_{ult}. The initial portion of a typical stress strain obtained for the test coupon is depicted in FIG. 3.4.

The variation between the highest and lowest values of the yield stress measured for section L amounted to approximately 15% of the lowest value. This variation is less than that for WF shapes where corresponding variations of 20% have been noted.

Residual strain distributions for sections E, F and L are shown in FIG. 3.5 and FIG. 3.6. The distributions were determined for one specimen of each of sections F and L and for three specimens of section E, as this gave the most severe distribution and the largest magnitude of strain. The measurements used to obtain the residual strains account for the curvature produced by the bowing action when the strips were cut free. Locations of the strips are shown in FIG. 3.3.

All sections showed the same general distribution of residual strain, with the exception of section F. In section F the strain values were relatively low and the resulting distribution may not be reliable.

The residual stress distribution must satisfy the three equations of equilibrium. These may be expressed as

$$\int \sigma_r dA = 0 \qquad 3.1$$

$$\int \sigma_r y dA = 0 \qquad 3.2$$

$$\int \sigma_r x dA = 0 \qquad 3.3$$

Equation 3.1 states that the net axial force on the section must be zero, while Equations 3.2 and 3.3 state that the moments due to the residual stresses about the x and y axes must be zero. The residual stress distributions computed from the measured residual strain distributions did not satisfy these equations exactly. The measured residual strain distributions were therefore adjusted before being used in computations.

The residual stress distribution obtained for section E was chosen as being the most severe expected for hot rolled hat shaped sections. This residual stress distribution was idealized as shown in FIG. 3.7. In FIG. 3.7, L1 represents the length of the flange, L2 the length of the web and L3 the length of the top of the hat. The lengths were measured on the center line of the section. The magnitude of the compressive stress in the flange tips, C, was selected on the basis of the measured values. With the specified value of C, and the known section geometry, the idealized distribution can be adjusted to comply with equations 3.1 and 3.2 by adjusting T and F. Equation 3.3 is satisfied by symmetry. T is the tensile stress in the flange and F the compressive stress in the top of the hat. The necessary computations were programmed for computer solution. Results obtained for sections E, F and L are given in Table 3.2.

TABLE 3.1 MATERIAL PROPERTIES FROM TESTS ON SECTION L

Strip Number	σ_y k.s.i.	$\varepsilon_y = \frac{\sigma_y}{E}$	ε_{st} ins/ins	E_{st} k.s.i.	ult k.s.i.	% elongation
1	56.4	0.00191	0.0128	646	84.1	22.5
2	53.2	0.00180	0.0107	603	83.4	20.5
3	53.5	0.00181	0.0163	540	81.5	19.7
4	50.6	0.00171	0.0067	700	81.7	15.2
5	49.2	0.00166	0.0068	681	83.4	17.3
6	53.0	0.00179	0.0152	500	80.7	18.0
7	52.1	0.00176	0.0083	760	82.5	21.3
8	54.1	0.00183	0.0156	740	84.3	19.2

Note E = 29,600 k.s.i.

TABLE 3.2 VALUES FOR BALANCED, IDEALIZED RESIDUAL STRESS DISTRIBUTION

Section	C k.s.i.	T k.s.i.	F k.s.i.
E	7.5	7.8	1.8
F	7.5	7.7	1.9
L	7.5	7.6	1.1

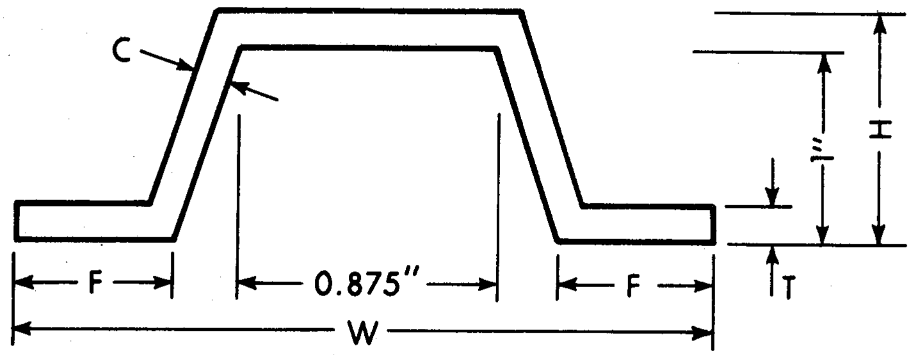

Dimension (ins)	Area	W	F	H	T	C
MIN	0.45	21/2	19/32	0.662	0.162	0.125
MAX	2.237	41/8	17/16	1.484	0.481	0.170

RANGE OF DIMENSIONS FOR ELEVEN SHALLOW HAT SECTIONS FROM MANUFACTURERS CATALOGUE

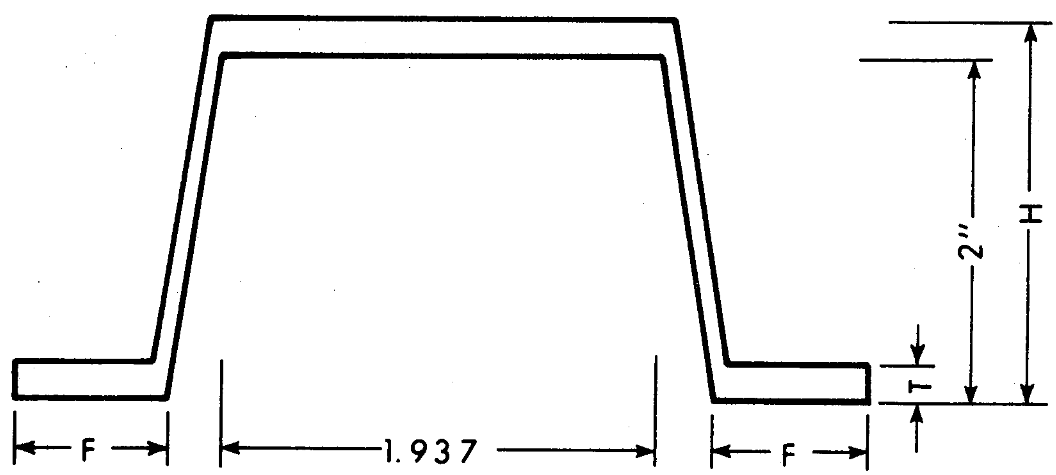

Dimension (ins)	Area	W	F	H	T	C
MIN	2.505	43/4	11/16	2.319	0.319	0.259
MAX	3.795	43/4	11/16	2.565	0.565	0.302

RANGE OF DIMENSIONS FOR FIVE DEEP HAT SECTIONS FROM MANUFACTURERS CATALOGUE

FIG. 3.1 DIMENSIONS OF HOT ROLLED HAT SHAPED SECTIONS

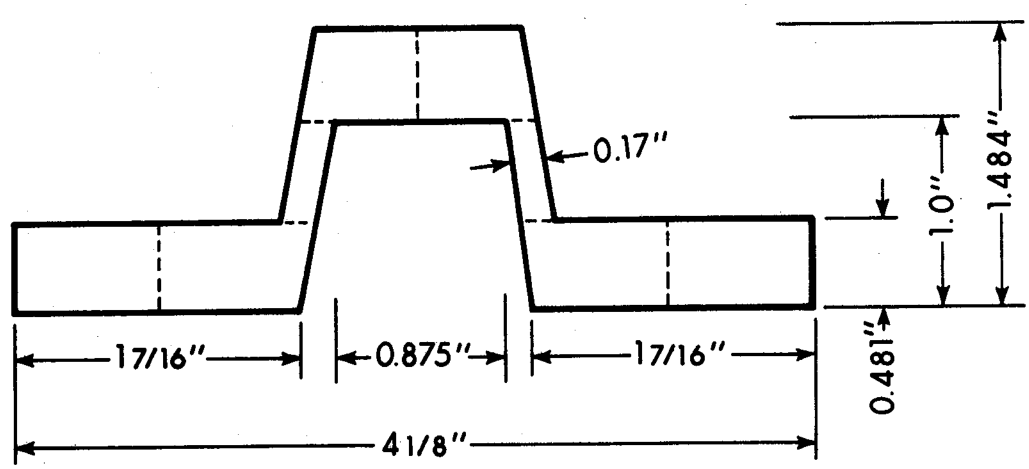

FIG. 3.2 SECTION L - DIMENSIONS TAKEN FROM MANUFACTURERS CATALOGUE

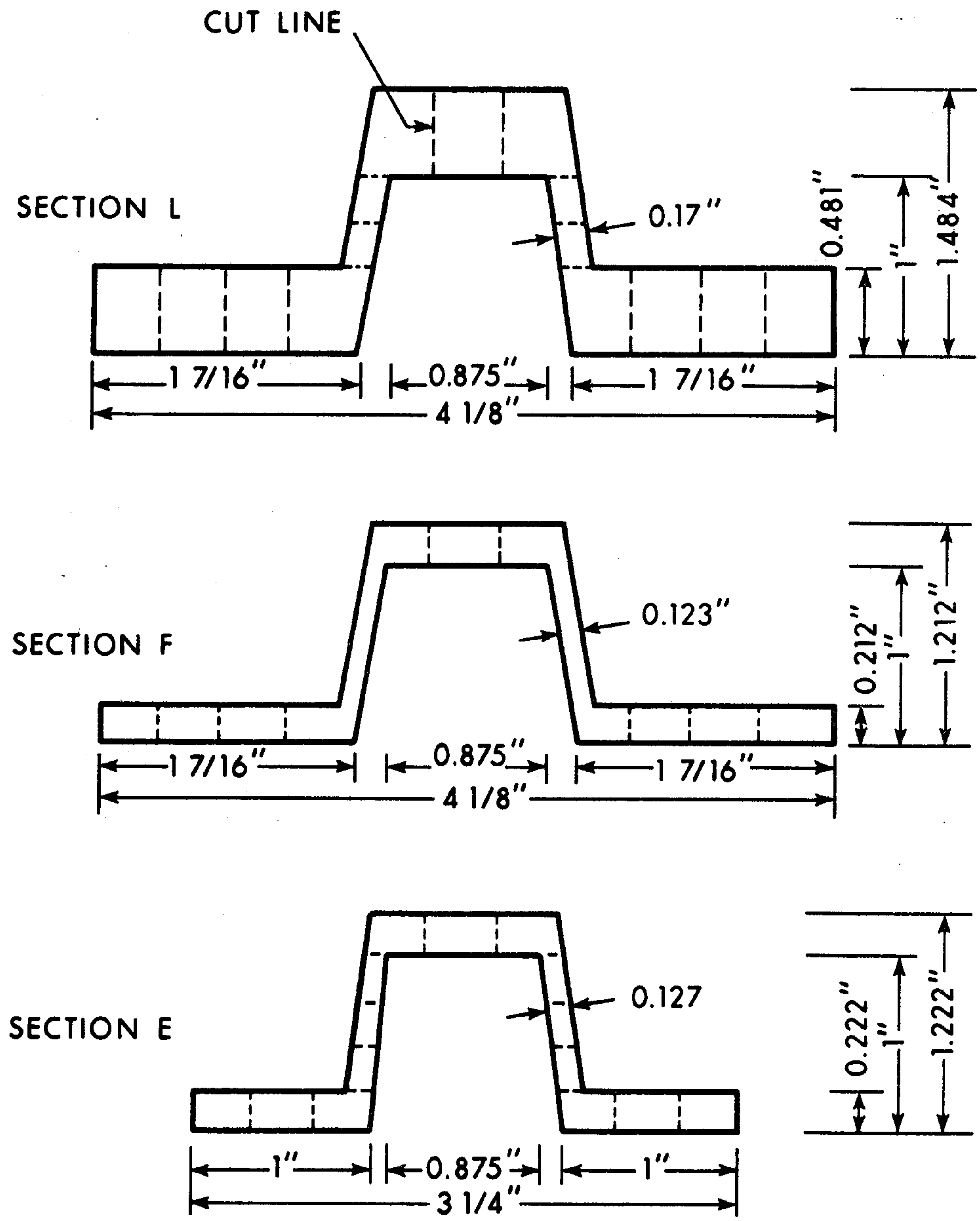

FIG. 3.3 SECTIONS E, F AND L - DIMENSIONS TAKEN FROM MANUFACTURERS CATALOGUE

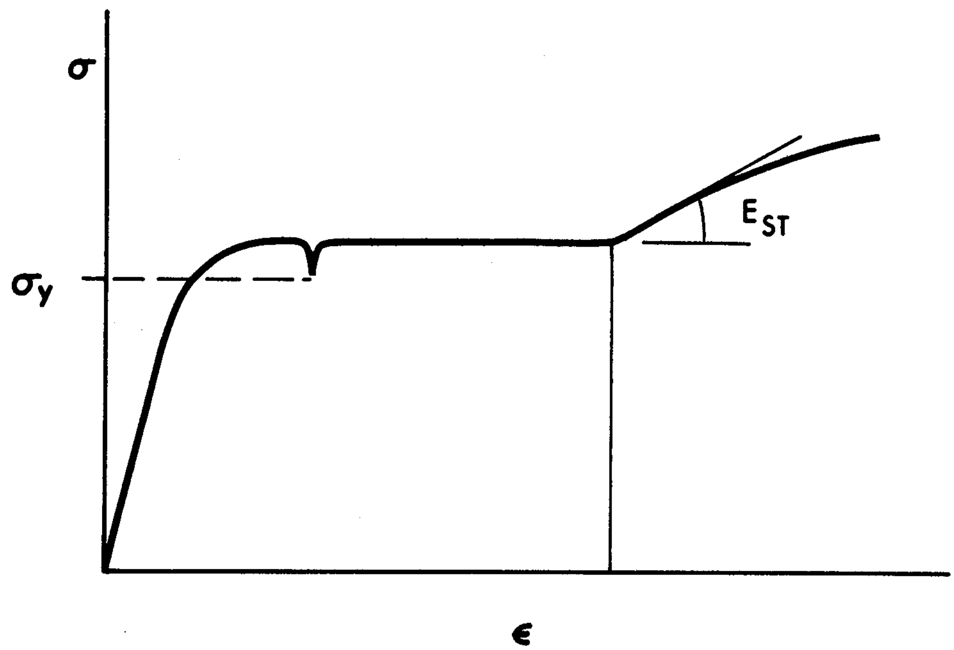

FIG. 3.4 INITIAL PORTION OF TYPICAL STRESS-STRAIN CURVE - SECTION L

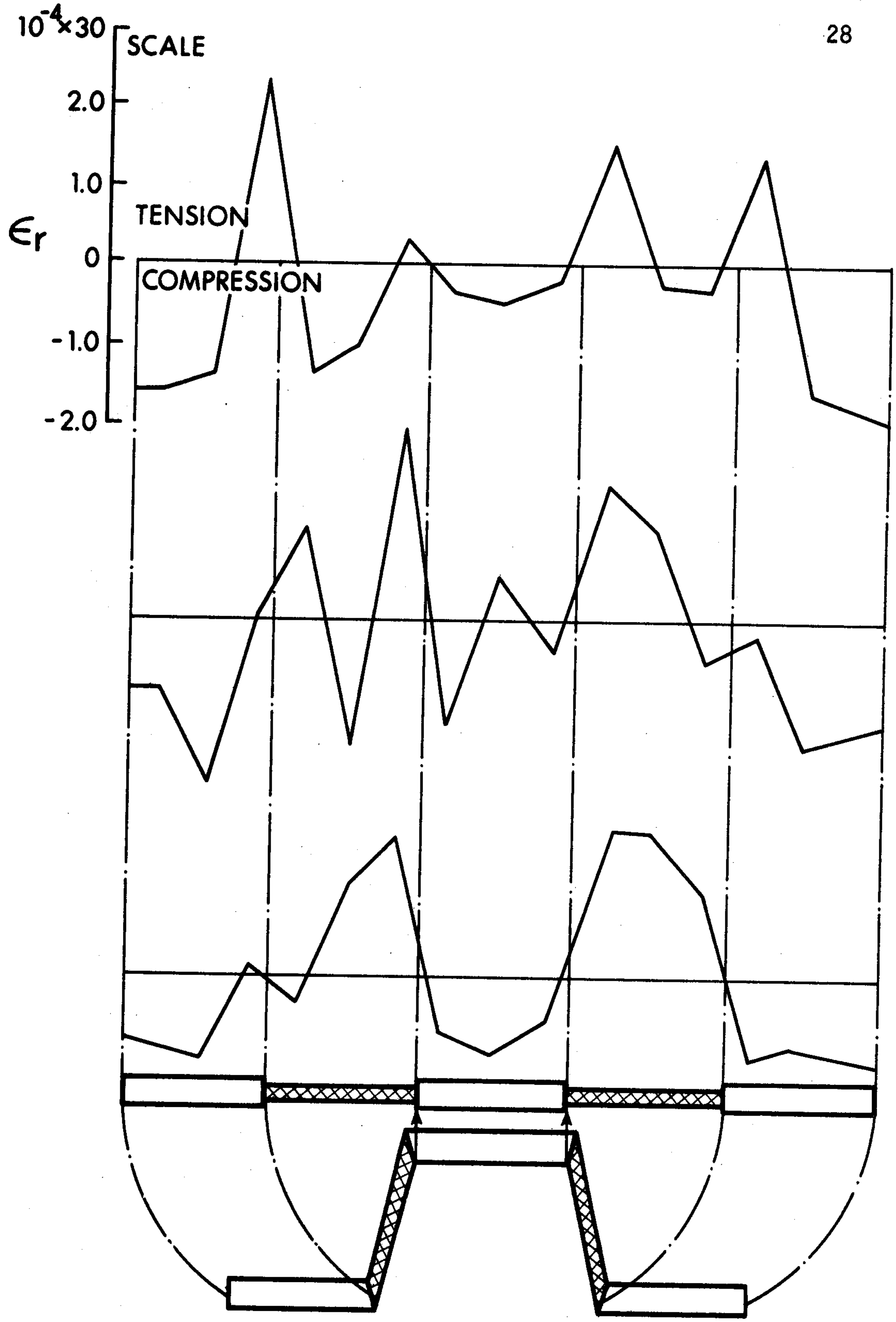

FIG. 3.5 RESIDUAL STRAINS - SECTION E

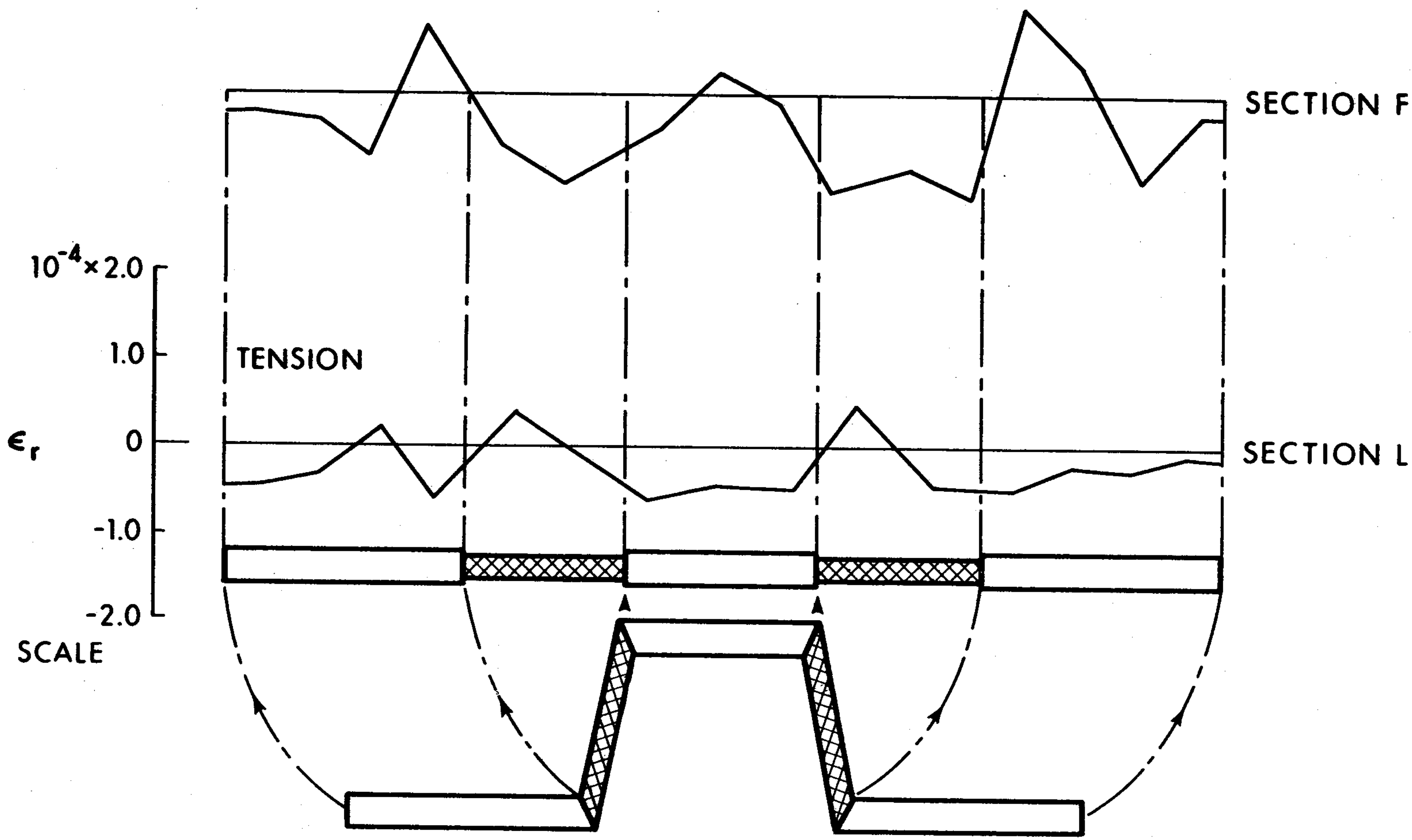

FIG. 3.6 RESIDUAL STRAINS - SECTIONS F AND L

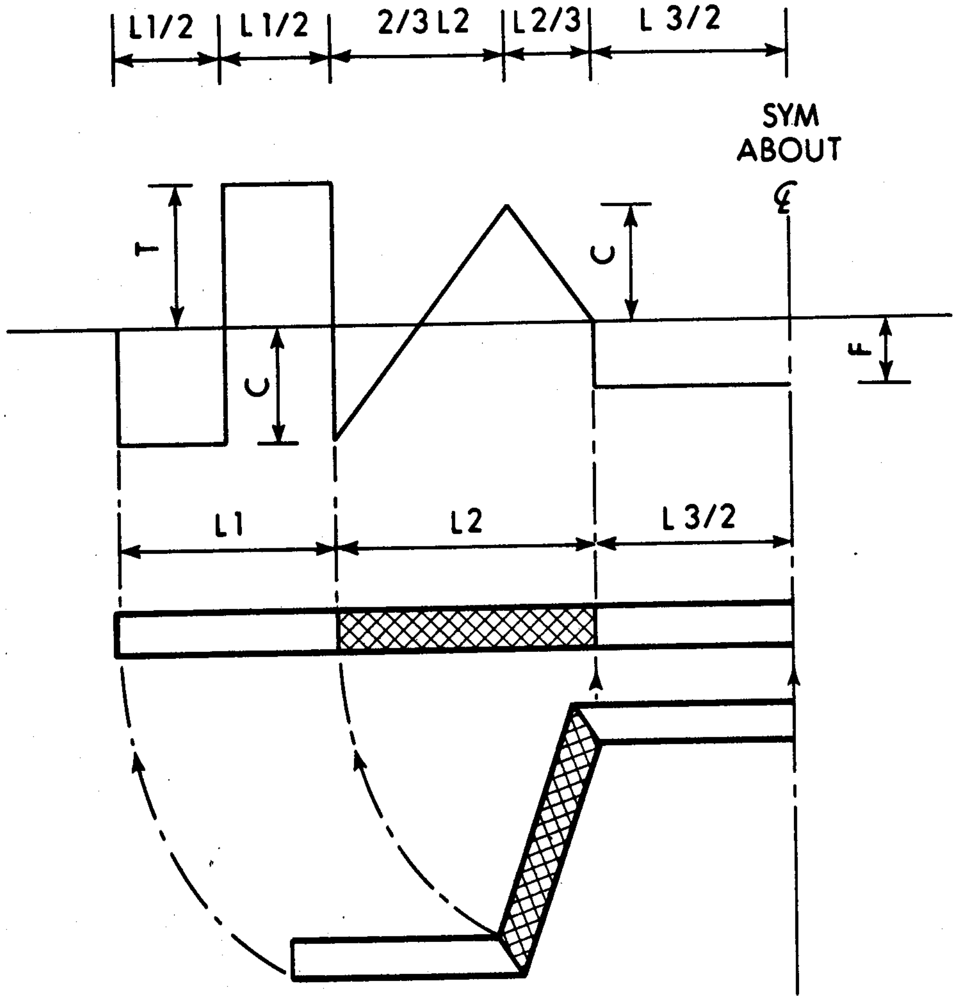

FIG. 3.7 IDEALIZED RESIDUAL STRESS DISTRIBUTION

CHAPTER IV

ANALYTICAL INVESTIGATION

The analytical investigation used Equations 2.7 and 2.8 to establish the critical lengths corresponding to flexural and lateral-torsional buckling. These equations are in terms of three unknowns; the load, the section properties and the critical length. Hence, any two of these quantities must be known before the equations can be solved. However, the section properties are influenced by the load, as the load level determines the extent of yielding in the section. The equations cannot, therefore, be solved directly.

Equations 2.7 and 2.8 were solved by first applying a uniform strain, ε_a, to the cross section as depicted in FIG. 4.1. The cross section was sub-divided into finite areas ΔA. Then, for any fibre, the total strain ε_t, is the sum of the residual and applied strains:

$$\varepsilon_t = \varepsilon_r + \varepsilon_a \qquad 4.1$$

The stress-strain relationship, FIG. 3.4, was entered with the total strain and the corresponding stress, σ, obtained. The stress in the fibre times the sub-area, summed over the cross section is equal to the applied load, P:

$$P = \sum_A \sigma \cdot \Delta A \qquad 4.2$$

The elastic core is defined by the total strain in each individual fibre. In the instant before buckling, the sub-areas are either elastic or plastic under the axial load. If the sub-area has yielded, it is assigned a zero thickness, if elastic, the actual thickness. For sub-areas strained into the strain-hardening region, the thickness t_i is given by:

$$t_i = t \frac{E_{st}}{E} \qquad 4.3$$

where t is the actual plate thickness. Section properties are then evaluated for the elastic core. However, K_T is based on the original area.(8)

With the section properties and axial load known, equations 2.7 and 2.8 can be solved for the lengths corresponding to flexural and lateral torsional buckling. The process was repeated with increasing values of the applied strain to trace the complete column curves. FIGURE 4.2 is a flow chart of the process, a listing of the computer program is included in Appendix A.

Three shallow hat sections, E, F and L were investigated. The residual strain distribution assumed was as shown in FIG. 3.7, however, three different assumptions were made for the yield stress distribution on the section. For one analysis, the yield stress was assumed to be constant at 55 k.s.i. over the cross section. In the second analysis the measured yield stresses for section L (Table 3.1) are used for the appropriate fibres. Finally a yield stress of 55 k.s.i. is used for the web plates and the yield stresses in the remaining plates, F_{YB}, are given by:

$$F_{YB} = 55 \times \frac{B}{W} \qquad 4.4$$

where B corresponds to the yield stress measured in the appropriate plate of Section L and W, to the yield stress measured in the web of Section L. This process is conservative as it implies that further reductions would be proportional to the changes in plate thickness; section L has the greatest variation in plate thickness.

The heaviest and highest deep hat sections, designated R and M in the manufacturers catalogue, and shown in FIG. 4.3 were also investigated. Deep hat sections showed a progressive increase in thickness from the lighter to the heavier sections. Therefore, the behaviour of R and M would represent limits on the range of behaviour for deep hat sections. The residual stress distributions were assumed to be as shown in FIG. 3.7. The yield stress distribution was assumed to be the same as that measured for the shallow hat sections. Section M was also analysed with an artifically higher yield stress in the web than in the remainder of the section.

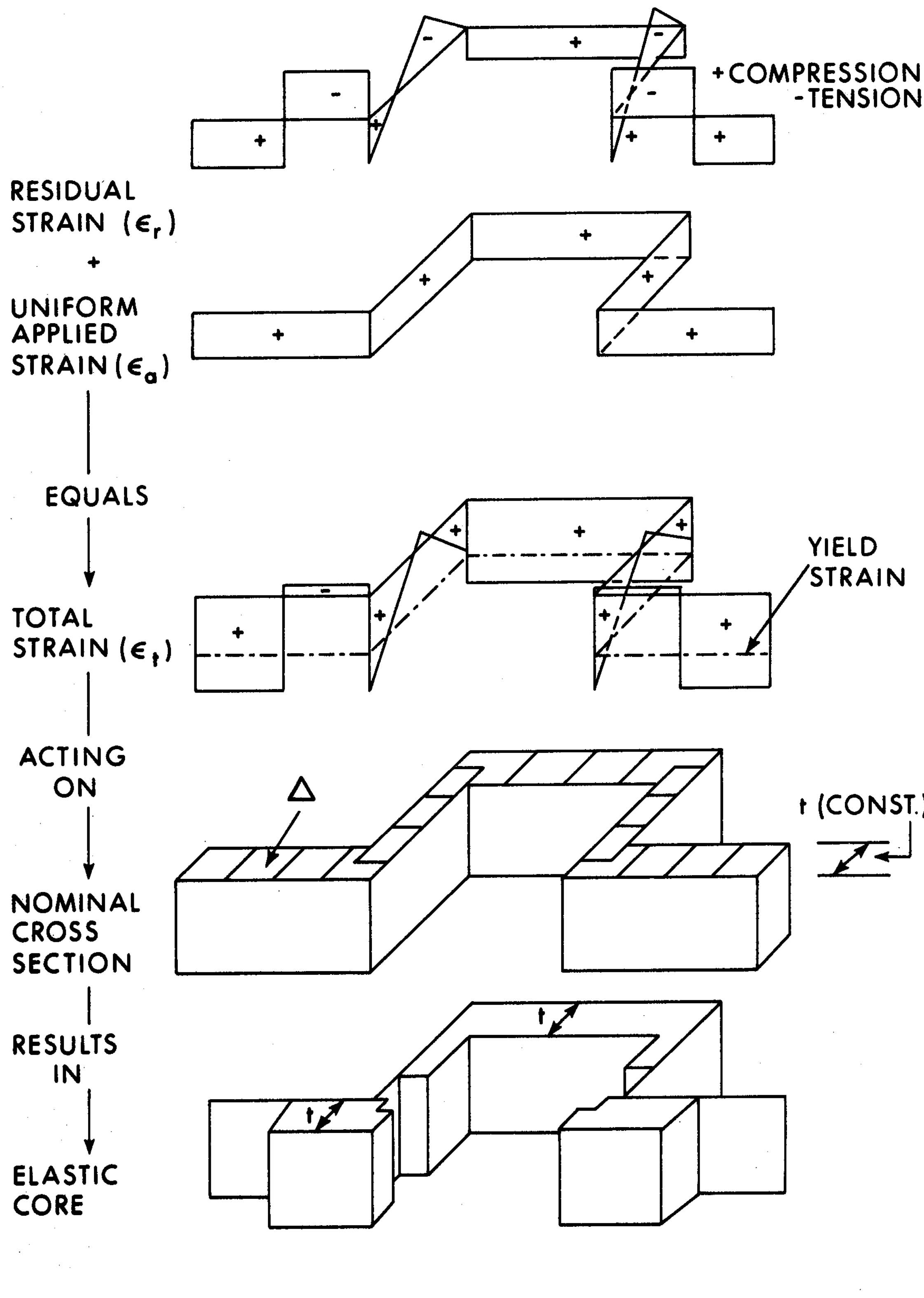

FIG. 4.1 CHANGE IN SECTION GEOMETRY UNDER APPLIED LOAD

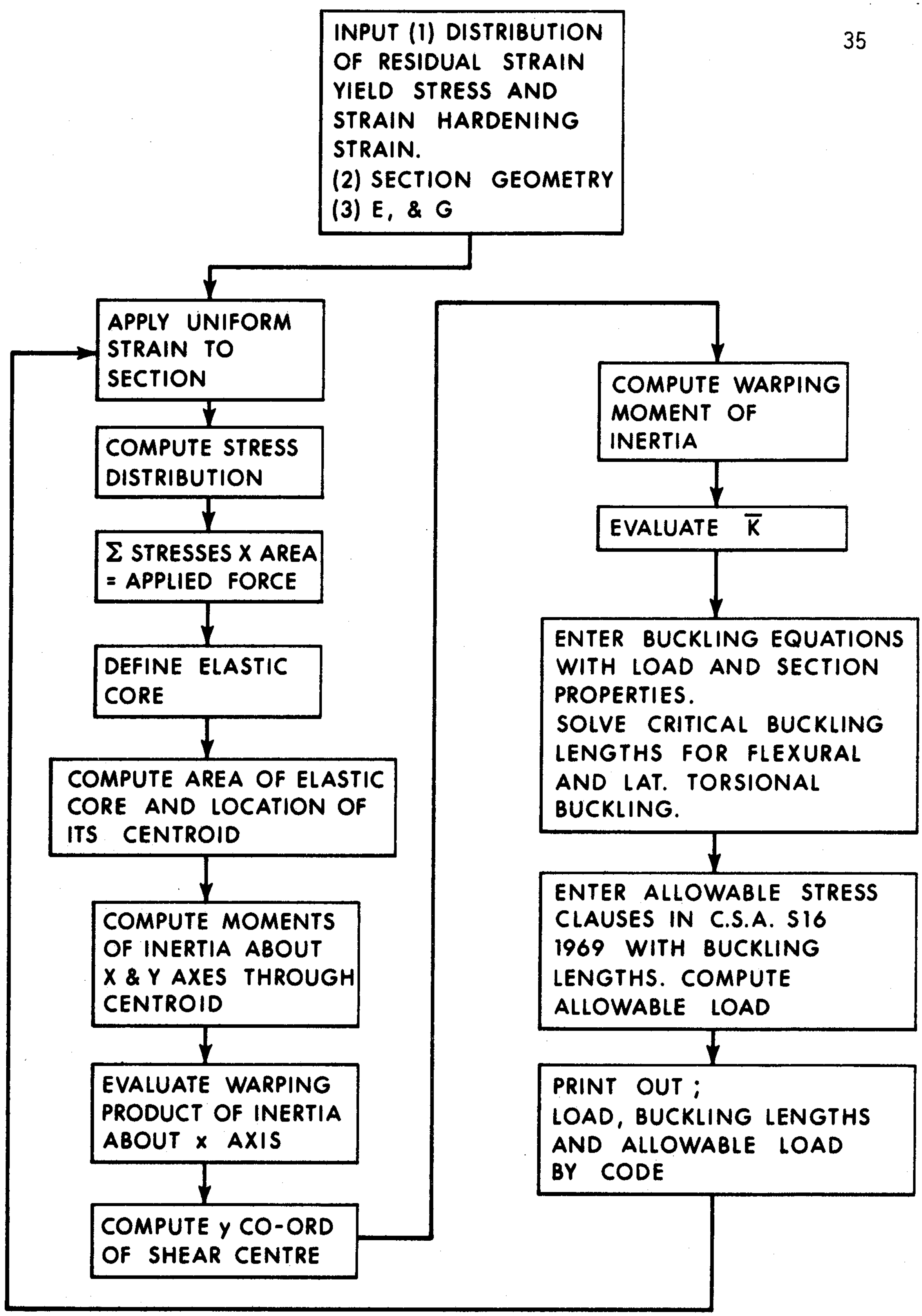

FIG. 4.2 FLOW CHART OF PROGRAM LOGIC

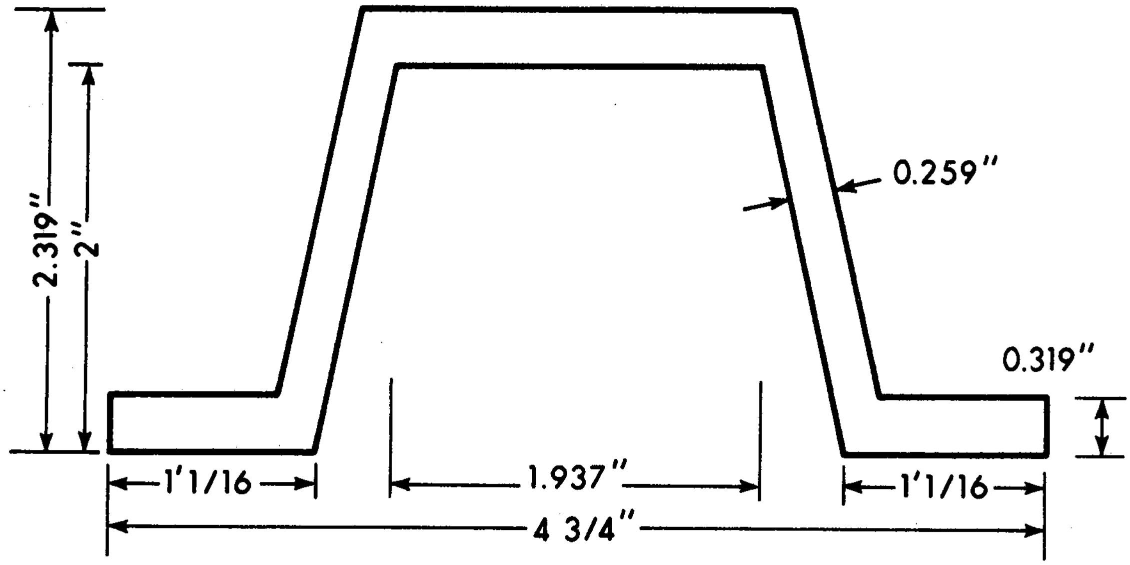

SECTION M

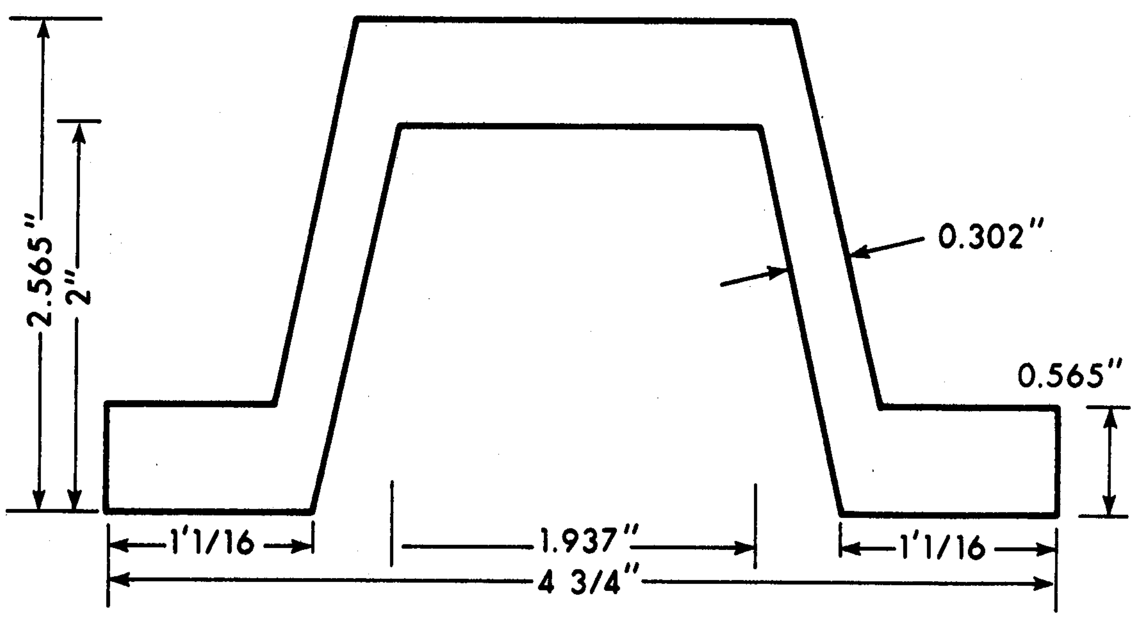

SECTION R

FIG. 4.3 SECTIONS M AND R DIMENSIONS TAKEN FROM MANUFACTURERS CATALOGUE

CHAPTER V

RESULTS

Column curves for the different sections analysed are given in FIGS. 5.1 to 5.5. These curves plot the relationships between the slenderness ratio, L/r_x, and the average applied stress at the instant of buckling, σ. The buckling stress has been non-dimensionalized as σ/σ_y, where σ_y is the weighted yield stress for the section and is given by:

$$\sigma_y = \frac{\int_A \sigma_{\bar{y}} \, dA}{A} \qquad 5.1$$

where $\sigma_{\bar{y}}$ is the yield stress on element dA, of the cross section, and A, is the area of the cross section.

The curves have the same general shape for all sections analysed. For a long, slender column, the maximum total strain at buckling is below the yield strain. More stocky columns buckle only after portions of the cross section have yielded and very short, or stub columns, unload only after complete yielding of the section.

FIGURE 5.1 plots the column curves for section E. The relationships for flexural buckling and for lateral-torsional buckling are plotted through the full range of column lengths (long, intermediate and short). For each mode of buckling, three different yield stress distributions were assumed as discussed above. The results for the longer columns, which buckled elastically, are independent of the yield stress distributions. In the inelastic range, the column curves were fairly similar under the assumption of a constant yield stress over the cross section and the assumption that the yield stress distribution was adjusted to produce a value of 55 k.s.i. in the web. The section having the measured yield stress distribution, however, had a reduced flexural buckling strength, as compared with the other two. The average of the measured yield stresses for this section was less than the average yield stress for the sections having the two assumed distributions; thus this section deteriorated more rapidly once yielding was initiated since the residual strains represented a higher proportion of the yield strain. In each figure the separation caused by the different yield stress distributions is emphasised by shading. FIGURES 5.2 and 5.3 show similar trends for sections F and L. For each section, the lowest buckling strengths were obtained for the measured yield stress distribution. The separation between the flexural and lateral-torsional buckling curves increased for the heavier sections, since the larger flanges increased the torsional resistance more than the flexural resistance.

All curves show a marked discontinuity due to the shape of the assumed residual strain distribution. The residual strains were assumed to be constant over the flanges and top of the hat section. Consequently, large areas of the cross-section yield simultaneously, producing a drastic reduction in flexural and torsional stiffness. The true residual strain distribution would be similar in shape to that assumed, but would probably vary somewhat over the plate length. Hence, under increasing axial load, progressive yielding of the section would occur, causing a gradual reduction in the buckling strength. The assumed residual strain distribution is probably more severe than the actual distribution, and the predicted buckling strengths are thus conservative.

For all sections analysed, the ultimate strength of the member was associated with the flexural buckling strength, regardless of the yield stress distribution assumed. The results obtained for the section having the measured distribution of yield stress and the adjusted distribution of yield stress, showed the least amount of spread between the flexural and lateral torsional buckling curves. For these distributions the yield stresses in most of the flange plate areas were lower than in the webs. Hence the flanges yielded at a relatively early stage of loading and, at this stage, the member acted as a narrow beam with a high flexural but a low torsional resistance.

The tendency for failure through lateral torsional buckling is increased for deep hat sections. FIGURES 5.4 and 5.5 plot column curves for sections M and R respectively. For these sections, the lateral torsional buckling strength is slightly lower than the flexural buckling strength over a small range of slenderness ratios. The tendency towards failure by inelastic lateral torsional buckling was further increased by assuming an artifically higher yield stress in the web of section M(60 k.s.i.) than in the rest of the section. FIGURE 5.4 plots the column curve for this case. The lateral torsional buckling strength is now slightly lower than the flexural buckling strength over a larger range of slenderness ratios. However, even in this extreme case, the ultimate strength of the member is very close to that associated with the flexural buckling strength. For the cases considered, the ultimate strength of hot rolled hat shaped column sections can be taken as the flexural buckling strength.

This conclusion implies that the allowable stress provisions of C.S.A. S16 1969 will provide the customary factors of safety against buckling. TABLE 5.1 lists the minimum factors of safety computed for the different sections.

The slenderness ratios listed in TABLE 5.1 represent the boundaries of the various provisions of C.S.A. S16 (0, C_o, C_p) and one intermediate point, which corresponds to the elastic limit $L/r_x = 78$. The location of these slenderness ratios is indicated in FIG. 5.7. In the elastic buckling range as defined by C.S.A. S16 ($L/r_x \geq C_p$) the factor of safety is 1.92 and once the section is completely yielded at $L/r_x = 0$, the factor of safety is 1.67. The factor of safety at $L/r_x = 78$ is greater than 1.92 since the residual strain distribution assumed by C.S.A. S16 is more severe than the measured distribution used in this investigation.

In each case considered, the factors of safety provide an adequate margin against buckling and justify the use of C.S.A. S16

1969 as a basis for design.

The analysis used to obtain the column curves assumes that the load is applied concentrically. However, the investigation showed that yielding of a portion of the cross-section is accompanied by a slight shift in the centroid of the elastic core. This process is depicted in FIG. 5.6 for one load increment. The axial load is applied through the original centroid C, until a limiting value of the axial load, P_{el}, is reached. Under a subsequent increment of axial load, ΔP, the section yields and the new centroid, C', is situated a distance e from the original centroid. The member is now subjected to an axial load of $P + \Delta P$ and a moment of $e \times \Delta P$. The magnitude of this moment, however, is small. TABLE 5.2 lists the values of e for section E. For this section P_{el} is 49.5 kips and, as the load is increased above this value, the centroid of the elastic core moves from its original position. Each increment of load therefore, induces a moment, as the load increments are no longer applied through the original centroid. Under the last increment of load the section is completely plastic. The total moment acting on the section at this stage is obtained by summing the moments induced by the individual load increments. For section E this total moment is 0.62 in. kips. This moment compares with the plastic moment capacity for the section of 16 in. kips, that is, the total moment is 2.5% of the plastic moment. The error caused by neglecting the effect of the shift of the centroid should be small.(12) Buckling strengths obtained from tests on 'T' sections compare closely with the theoretically predicted strengths under similar conditions.[12] The comparison showed that for practical purposes, the shift of the centroid could be neglected.

Section	Slenderness Ratio 0	$C_0 = 19$	78	$C_p = 82$
E	1.67	1.67	2.1	1.92
F	1.67	1.67	2.1	1.92
L	1.67	1.67	2.1	1.92
M	1.67	1.67	2.1	1.92
R	1.67	1.67	2.1	1.92

TABLE 5.1 FACTORS OF SAFETY PROVIDED BY C.S.A. S16 1969 AGAINST BUCKLING

Total Load kips	Load Increment ΔP (kips)	Distance from top of hat to centroid	Shift in centroid e (ins)	Applied Moment $e \times \Delta P$
49.5		0.69		
52.4	3.9	0.75	0.06	0.23
53.9	1.5	0.76	0.07	0.10
55.2	1.3	0.76	0.08	0.10
56.4	1.2	0.85	0.16	0.19

Total Moment = 0.62 ins. kips

TABLE 5.2 SHIFT OF CENTROID SECTION F

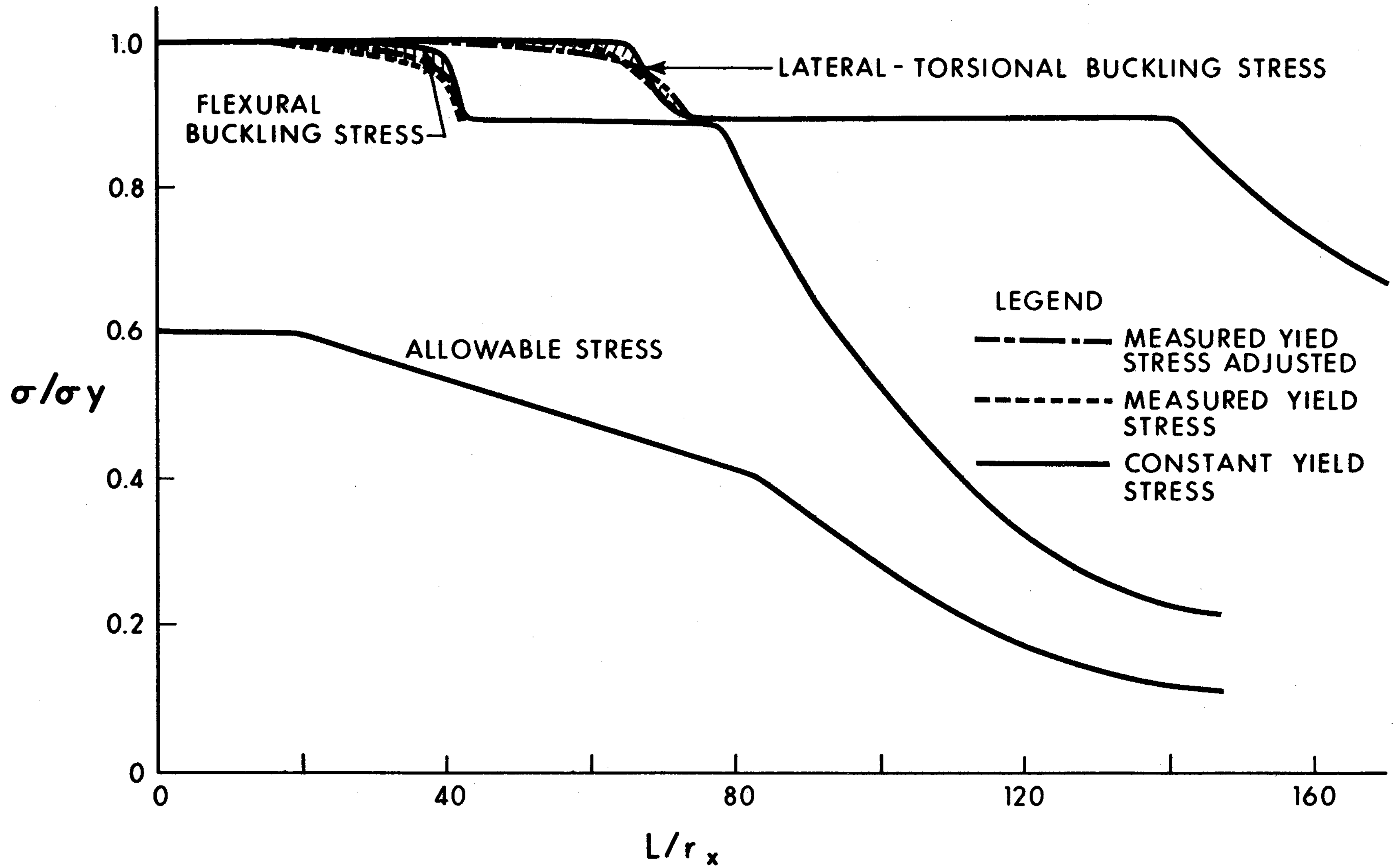

FIG. 5.1 COLUMN CURVE - SECTION E

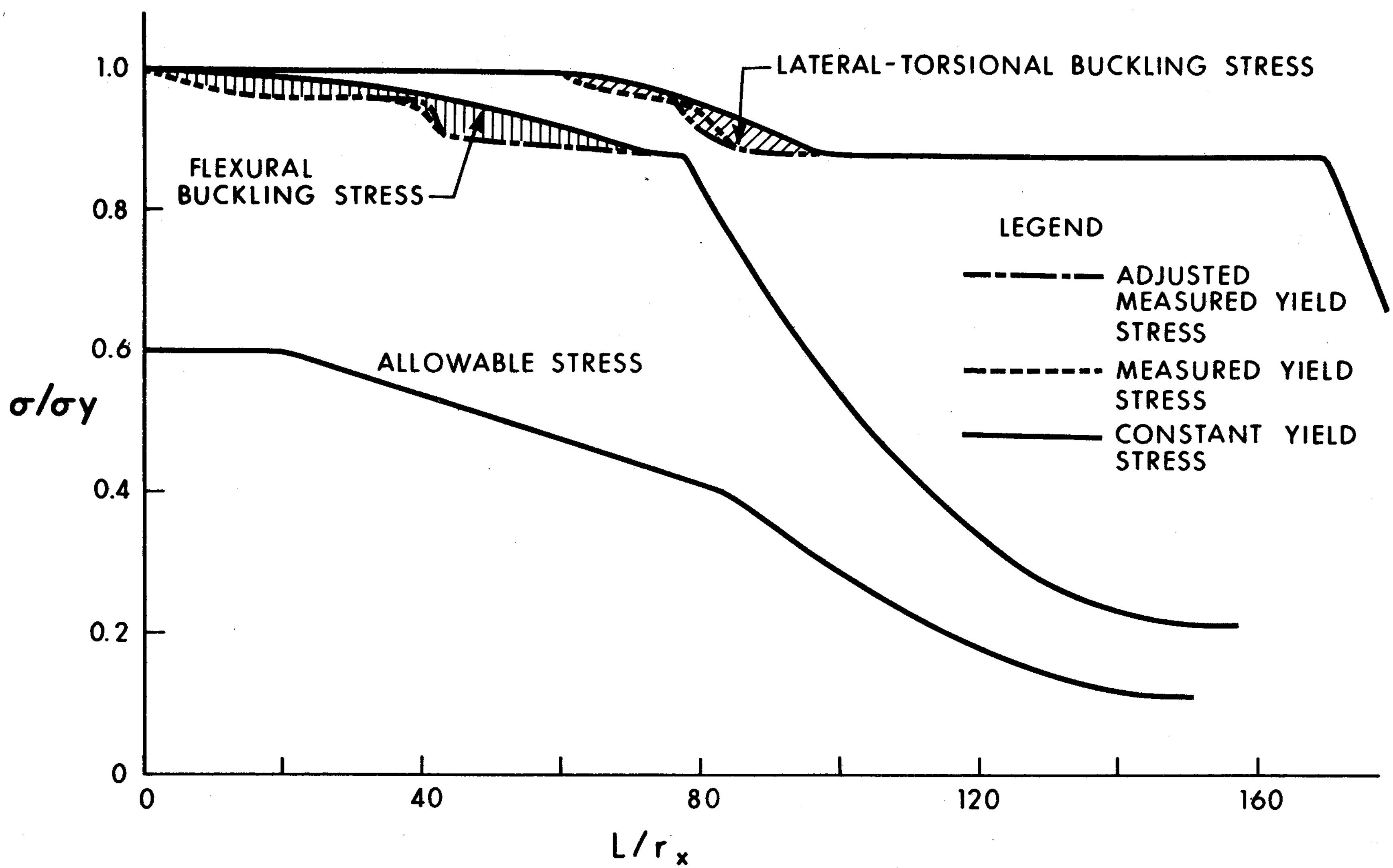

FIG. 5.2 COLUMN CURVE - SECTION F

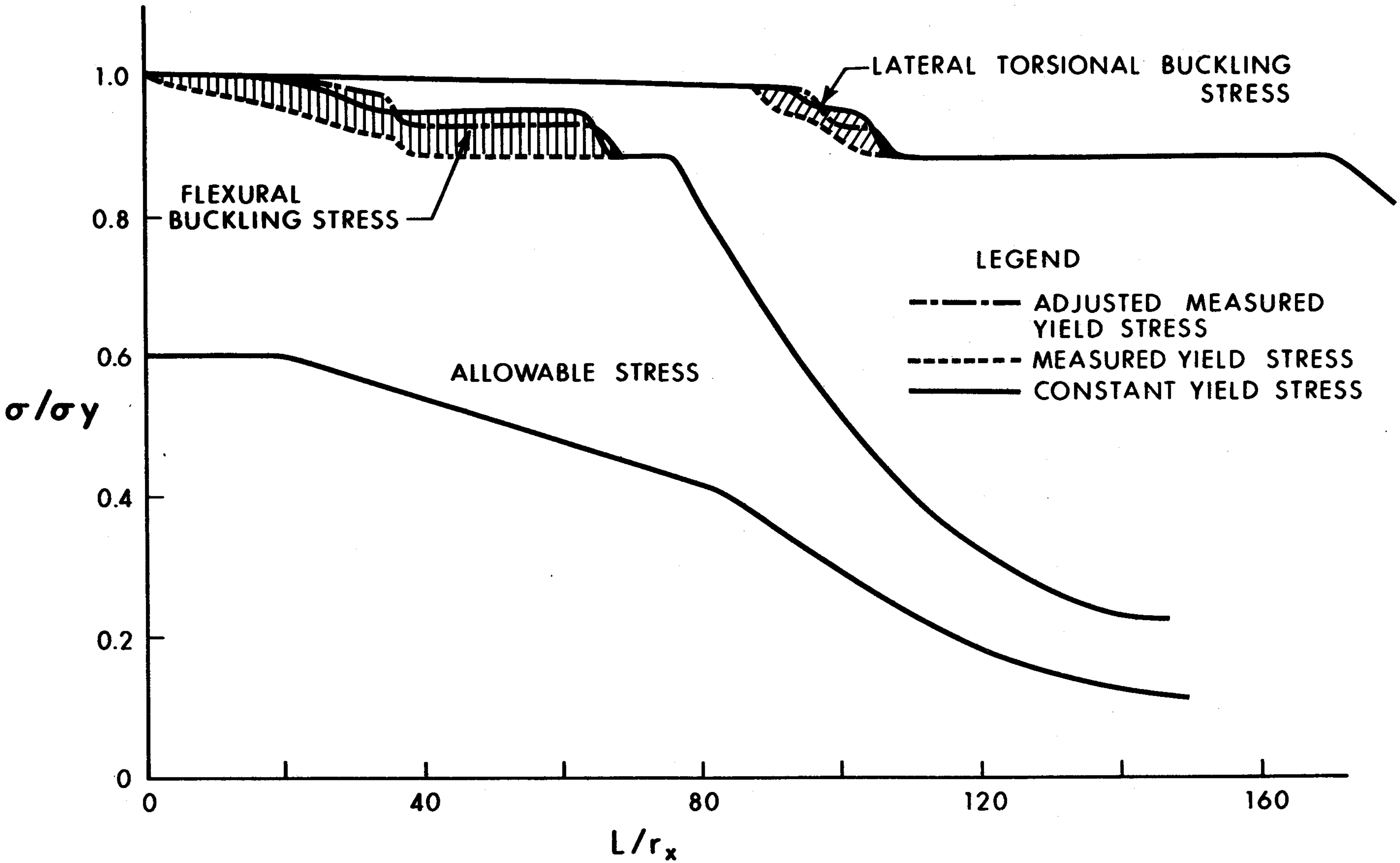

FIG. 5.3 COLUMN CURVE - SECTION L

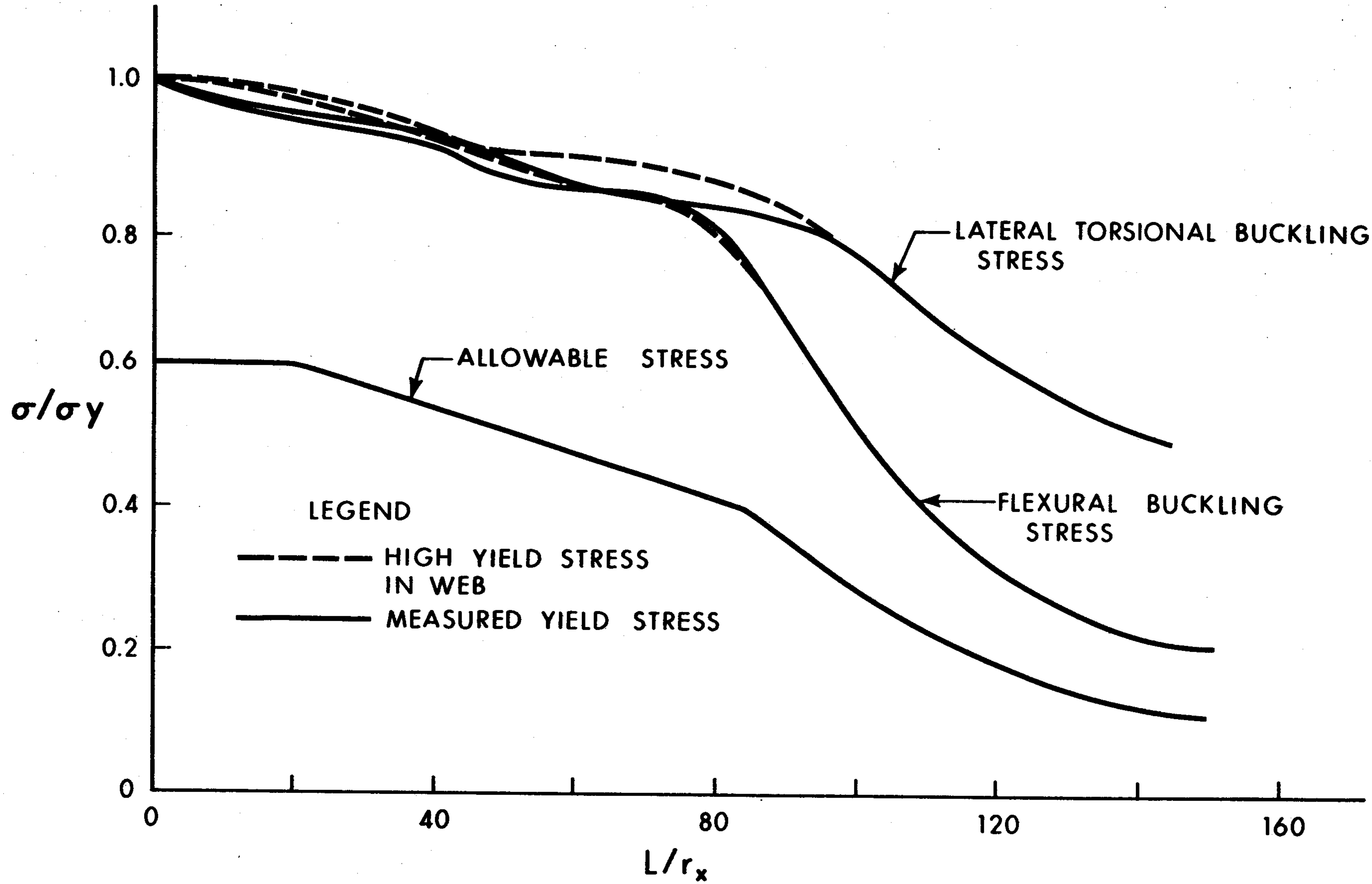

FIG. 5.4 COLUMN CURVE - SECTION M

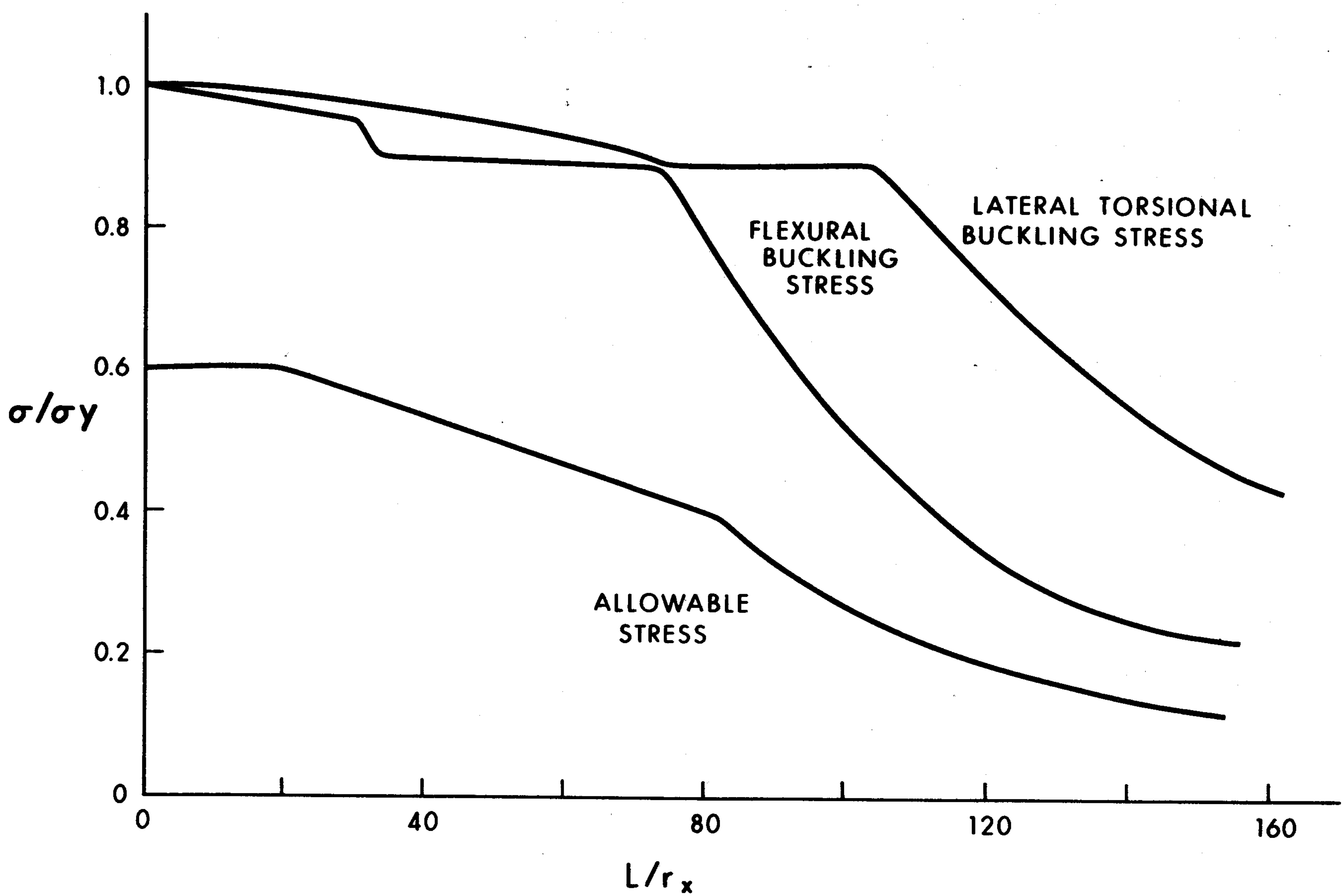

FIG. 5.5 COLUMN CURVE - SECTION R

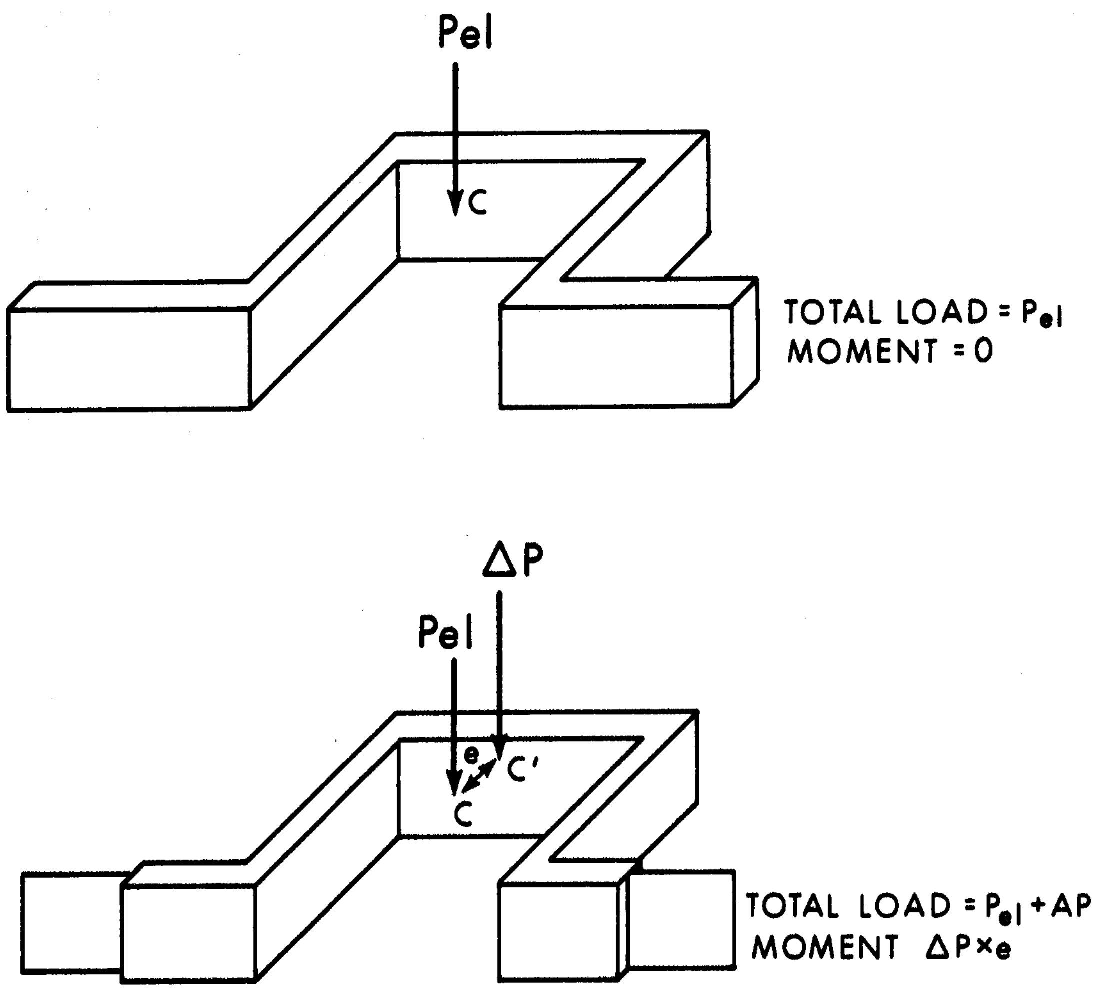

FIG. 5.6 SHIFT OF CENTROID ON YIELDING

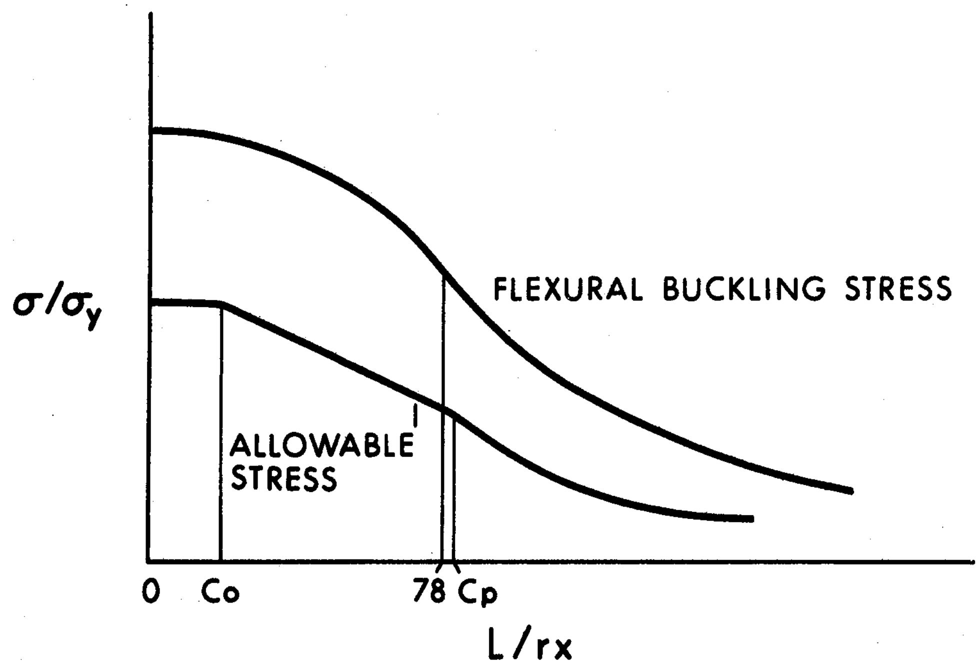

FIG. 5.7 SLENDERNESS RATIOS USED IN TABLE 5.2

CHAPTER VI

SUMMARY AND CONCLUSIONS

Hot rolled hat shaped sections are commonly used as chord members for open web steel joists. The chord member may be idealized as a series of pin ended axially loaded segments. The ultimate strength of a segment is assumed to be given by its buckling strength. As the section has only one axis of symmetry, buckling may occur in either a flexural or a lateral torsional mode.

Residual strains were measured for the hat shaped sections using the method of sectioning, but allowing for the bowing action of the strips on release. With the residual strains known, a step by step procedure, based on the tangent modulus approach, was used to obtain column curves for the different sections. The column curves covered the practical range of slenderness ratios and considered the effect of variations in the yield stress distribution on the buckling strength.

The measured residual strains were small, with maximum compression values of approximately 0.00025 inches per inch. The idealized residual strain distribution assumed constant compressive strains over the flange tips, which caused discontinuities in the column curves as these areas yielded. However, the idealized distribution furnishes conservative results as it envelopes the actual distribution.

A lower bound on the buckling strength resulted from the consideration of the actual (measured) yield stress distribution. The residual strains represented a greater proportion of the average yield strain for this distribution and so deterioration of the section in the inelastic range was more rapid than for the other idealized distributions.

The column curves were based on the tangent modulus concept recommended by the Column Research Council. Column curves obtained using this concept showed that the flexural buckling strength was generally less than the lateral torsional buckling strength. Exceptions to this rule were found to exist over very small ranges of slenderness ratio and only under extreme conditions. The allowable stress provisions contained in C.S.A. S16 1969 resulted in adequate factors of safety against buckling; the use of these provisions for design of hot rolled hat shaped sections is justified.

The investigation assumed that the ultimate strength of the member corresponds to its buckling strength and did not consider the effects of the lateral loads and end restraints on the ultimate strength of the member.

LIST OF REFERENCES

1. Winter, G. and Uribe, J. - "Effects of Cold Work on Cold Formed Steel Members" Symposium on Thin Walled Steel Structures - Their Design and Use, University College of Swansea, September 1967.
2. Timoshenko, S. - "Strength of Materials - Part II" Van Nostrand Co., New York, 2nd Edition, 1956.
3. Beedle, L.S. et al - "Structural Steel Design", Ronald Press Co., New York, 1964.
4. Bleich, F. - "Buckling Strength of Metal Structures", McGraw-Hill Book Co., New York, 1952.
5. Galambos, T.V. - "Structural Members and Frames", Prentice-Hall International Series in Theoretical and Applied Mechanics, Englewood Cliffs, N.J., 1968.
6. Sherman, D. - "Measurement of Residual Stresses in Tubular Members", Proc. ASCE, Vol. 95, ST4, April 1969.
7. "Guide to Design Criteria for Metal Compression Members", Edited by B.G. Johnson, 2nd Edition, John Wiley & Sons Inc., New York, 1966.
8. Lee, G.C., Fine, D.S. and Hastreiter, W.R. - "Inelastic Torsional Buckling of H Columns", Proc. ASCE, Vol. 93, ST5, October 1967.
9. Chajes, A. and Winter, G. - "Torsional Flexural Buckling of Thin Walled Members", Proc. ASCE, Vol. 91, ST4, August 1965.

10. Pekoz, T.B. and Winter, G. - "Torsional Flexural Buckling of Thin Walled Sections Under Eccentric Loading", Proc. ASCE, Vol. 95, ST5, May 1969.

11. McDonald, W.S. and Lenzen, K.H. - "Inelastic Behaviour of the Compression Chord of Open Web Steel Joists", Studies in Engineering Mechanics, Report No. 24, University of Kansas, Lawrence, Kansas, 1966.

12. Nishino, F. - "Buckling Strength of Columns and Their Component Plates", Fritz Engineering Laboratory Report No. 290.10, Lehigh University, Bethlehem, PA., 1964.

ACKNOWLEDGEMENTS

This study is an extension of a project initiated to investigate the load carrying capacity of double angle columns, in progress at the Department of Civil Engineering, University of Alberta. P.F. Adams is the Project Director. The project is sponsored financially by the Canadian Steel Industries Construction Council, with technical assistance from the Canadian Institute of Steel Construction.

The assistance of H.A. Krentz, Director of Research and Development, C.I.S.C. and A.J.M. Aikman, Alberta Regional Engineer, C.I.S.C., is particularly acknowledged. The cooperation and interest of A. Turnbull, and other staff members of Great West Steel Industries Ltd., is also acknowledged. Great West Steel Industries Ltd., also supplied the specimens used for the determination of the material properties.

The assistance of J. McLean and members of the Civil Engineering Staff in the performance of the testing program, and Miss H. Wozniuk who typed the report, is acknowledged. B. Constant assisted in writing the computer program.

```
LEVEL 17 ( 1 NOV 68)                    OS/360  FORTRAN H                    DATE  70.190/12.03.43

         COMPILER OPTIONS - NAME=  MAIN,OPT=02,LINECNT=59,SOURCE,EBCDIC,NOLIST,NODECK,LOAD,NOMAP,NOEDIT,ID,NOXPFF
  ISN 0002              DIMENSION T(5),ST(50,50),SR(50,50),A(50,50),XC(100),YC(100),W(100)
                       1,ROE(50,50),FF(50,50),ROEO(50,50),WO(50),STRESY(50,50),WN(50),SS(5
                       20,50),SY(50,50),XO(50,50)
  ISN 0003              INTEGER OUTPUT,D(5),B,P,D1,D2,D3,DIV1,DIV2A,DIV2B,DIV3A,DIV3B,DD1,
                       1DDD2,DD2,DDD3,DD3,DD4,DD5,DDD5
  ISN 0004              REAL L1,L2,L3,L(5),LI,LOAD,IXII,IYII,IX(50,50),IY(50,50),IXBAR,
                       1IYBAR,IXBART,IYBART,IWX,IWY,KT,IW
  ISN 0005              REAL LL(3)
  ISN 0006              REAL LX,LLL,KLR
                  C     DEFINE INPUT AND OUTPUT UNIT NUMBERS
  ISN 0007              INPUT = 5
  ISN 0008              OUTPUT = 6
                  C
                  C     READ ALL MATERIAL PROPERTIES
                  C
  ISN 0009              READ(INPUT,1) E , ES
  ISN 0010            1 FORMAT (2F10.2)
                  C
                  C     READ MEMBER SIZES IN INCHES AND DIVISIONS REQUIRED
                  C
  ISN 0011              READ(INPUT,2) T(1),T(2),T(3),L(1),L(2),L(3),D(1),D(2),D(3),ANGLE
  ISN 0012            2 FORMAT (6F10.5,3I5,F5.2)
                  C     L=LENGTH OF SECTION, T= THICKNESS OF SECTION, D= NO. OF DIVISIONS
  ISN 0013              THETA = ANGLE / 57.29578
  ISN 0014              ALPHA = 3.14159/2. - THETA
  ISN 0015              DO 5 I=1,3
  ISN 0016              P = D(I)
  ISN 0017              READ (INPUT,11) (STRESY(I,K),SS(I,K), K=1,P)
  ISN 0018           11 FORMAT (2F10.7)
  ISN 0019            5 CONTINUE
                  C
                  C     READ IN RESIDUAL STRAINS FOR EACH DIVISION,COMPRESSION POSITIVE
                  C
  ISN 0020              DO 2001 I=1,3
  ISN 0021              P = D(I)
  ISN 0022              READ (INPUT,4) (SR(I,K), K=1,P)
  ISN 0023            4 FORMAT (8F10.8)
  ISN 0024         2001 CONTINUE
  ISN 0025              READ(5,500)G,SSS
  ISN 0026          500 FORMAT(F8.1,F5.1)
                  C
                  C     READ ONE VALUE OF APPLIED STRAIN
                  C
  ISN 0027            3 READ (INPUT,6,END=999)SA
  ISN 0028            6 FORMAT (F10.8)
  ISN 0029              AIXT = 0.0
  ISN 0030              AYBART = 0.0
  ISN 0031              IXBART = 0.0
  ISN 0032              IYBART = 0.0
  ISN 0033              LOAD = 0.0
  ISN 0034              WRITE (OUTPUT,7)
  ISN 0035            7 FORMAT ( '1',51X,'CIVIL ENGINEERING DEPARTMENT'/ 54X ,
                       1 'UNIVERSITY OF ALBERTA'// 40X,'ANALYSIS OF RESIDUAL STRAINS IN HA
                       2T MEMBERS'/)
  ISN 0036              WRITE (OUTPUT,8) E,ES
  ISN 0037            8 FORMAT ( 20X,'MATERIAL PROPERTIES' / 9X,'MODULUS OF ELASTICITY = '
                       1,F10.2,' KSI' / 9X, 'STRAIN HARDENING MODULUS = ',F10.2,' KSI')
```

```
ISN 0038          WRITE (OUTPUT,9) (I,L(I),T(I),D(I), I=1,3), ANGLE
ISN 0039        9 FORMAT (20X,'DIMENSIONS AND GEOMETRY OF SECTION' //9X,'SECTION',
                 110X,'LENGTH',10X,'THICKNESS',10X,'NUMBER OF DIVISIONS'// 3(8X,I5,
                 29X,F10.5,6X,F10.5,17X,I5/)// 9X,'ANGLE = ',F5.2,'DEGREES'//)
ISN 0040          WRITE (OUTPUT,10) SA
ISN 0041       10 FORMAT( '1',45X,'APPLIED STRAIN = ',F10.8,' IN/IN' //20X,'TOTAL ST
                 1RAIN IN SECTION DUE TO APPLIED AND RESIDUAL STRAIN' // 2X,'SECTION
                 2',5X,'DIVISION',5X,'IX OF',8X,'IY OF',8X,'TOTAL',10X,'AREA',11X,'A
                 3YBAR',9X,'YIELD STRESS',4X,'STRAIN AT'/2X,'NUMBER',7X,'NUMBER',7X,
                 4'DIVISION',5X,'DIVISION',5X,'STRAIN',9X,'DIVISION',7X,'DIVISION',6
                 5X,'DIVISION',9X,'S HARDENING'/)
ISN 0042          DO 200 I = 1,3
ISN 0043          P = D(I)
ISN 0044          DD = D(I)
ISN 0045          DUM1 = T(I)*L(I)/DD
ISN 0046          DO 100 K=1,P
            C
            C     A(I,K) = AREA OF DIVISION K SECTION I
            C
ISN 0047          SY(I,K) = STRESY(I,K)/E
ISN 0048          ST(I,K) = SA + SR(I,K)
ISN 0049          IF (ST(I,K).LT.SY(I,K)) GO TO 40
ISN 0051          IF (ST(I,K).GT.SS(I,K)) GO TO 50
ISN 0053          XQ(I,K)=0.0
ISN 0054          LOAD = LOAD + 2.*STRESY(I,K)*DUM1
ISN 0055          A(I,K) = 0.00
            C     IX(I,K) = MOMENT OF INERTIA ABOUT OWN X AXIS
            C     IY(I,K) = MOMENT OF INERTIA ABOUT OWN Y AXIS
ISN 0056          IX(I,K) = 0.00
ISN 0057          IY(I,K) = 0.00
ISN 0058          GO TO 75
ISN 0059       40 XQ(I,K)=1.0
ISN 0060          A(I,K) = DUM1
            C     AIXT =  TOTAL AREA - FOR USE IN CALCULATION OF CENTROID
ISN 0061          AIXT = AIXT + A(I,K)
ISN 0062          LOAD = LOAD + 2.*E*ST(I,K)*DUM1
ISN 0063          GO TO 55
ISN 0064       50 XQ(I,K)=ES/E
ISN 0065          A(I,K)=DUM1*XQ(I,K)
ISN 0066          AIXT = AIXT + A(I,K)
ISN 0067          LOAD = LOAD + 2.*DUM1*(STRESY(I,K)+(ST(I,K)-SS(I,K))*ES)
ISN 0068       55 IF (I.EQ.2) GO TO 70
ISN 0070          IX(I,K) = L(I)/DD*(T(I)**3)/12.*XQ(I,K)
ISN 0071          IY(I,K) = T(I)*(L(I)/DD)**3/12.*XQ(I,K)
ISN 0072          GO TO 60
ISN 0073       70 IX(I,K) = T(I)*L(I)/DD*(T(I)**2*(SIN(THETA))**2 + (L(I)/DD)**2*(CO
                 1S(THETA))**2)/12.*XQ(I,K)
ISN 0074          IY(I,K) = T(I)*L(I)/DD*(T(I)**2*(SIN(ALPHA))**2 + (L(I)/DD)**2*(CO
                 1S(ALPHA))**2)/12.*XQ(I,K)
ISN 0075          F = K
ISN 0076          YBARD = L(I)/DD*(DD-F+0.5)*COS(THETA)
ISN 0077          AYBAR = A(I,K)*YBARD
ISN 0078          AYBART = AYBART + AYBAR
ISN 0079          GO TO 75
ISN 0080       60 IF (I.EQ.3) GO TO 75
ISN 0082          L2 = L(2)
ISN 0083          AYBAR = A(I,K)*L2*COS(THETA)
```

```
ISN 0084          AYBART = AYBART + AYBAR
ISN 0085       75 WRITE (OUTPUT,76) I,K,IX(I,K),IY(I,K),ST(I,K),A(I,K),AYBAR,STRESY(
                 1I,K),SS(I,K)
ISN 0086       76 FORMAT (2X,I5,7X,I5,10X,F10.8,3X,F10.8,3X,F10.8,5X,F10.8,5X,F10.8,
                 14X,F10.2,6X,F10.8//)
ISN 0087      100 CONTINUE
ISN 0088      200 CONTINUE
ISN 0089          YBAR = AYBART/AIXT
ISN 0090          WRITE (OUTPUT,111) YBAR
ISN 0091      111 FORMAT (9X,'YBAR = ',F10.4,' IN.'//)
ISN 0092          DO 400 I=1,3
ISN 0093          P = D(I)
ISN 0094          DO 300 K=1,P
ISN 0095          F = K
ISN 0096          DD = D(I)
ISN 0097          IF (I.EQ.1) GO TO 105
ISN 0099          IF (I.EQ.2) GO TO 110
ISN 0101          IXBAR = (IX(I,K)+A(I,K)*YBAR**2)*2.
ISN 0102          IYBAR = (IY(I,K)+A(I,K)*(L(I)/DD*(DD-F+0.5))**2)*2.
ISN 0103          GO TO 115
ISN 0104      105 L2 = L(2)
ISN 0105          IXBAR = (IX(I,K)+A(I,K)*(L2*COS(THETA)-YBAR)**2)*2.
ISN 0106          L3 = L(3)
ISN 0107          IYBAR = (IY(I,K)+A(I,K)*(L3+L2*SIN(THETA)+L(I)/DD*(DD-F+0.5))**2)*
                 12.
ISN 0108          GO TO 115
ISN 0109      110 L3 = L(3)
ISN 0110          IXBAR =(IX(I,K)+A(I,K)*(L(I)/DD*(DD-F+0.5)*COS(THETA)-YBAR)**2)*2.
ISN 0111          IYBAR = (IY(I,K)+A(I,K)*(L(I)/DD*(DD-F+0.5)*SIN(THETA)+L3)**2)*2.
ISN 0112      115 IXBART = IXBART + IXBAR
ISN 0113          IYBART = IYBART + IYBAR
ISN 0114      300 CONTINUE
ISN 0115      400 CONTINUE
ISN 0116          WRITE (OUTPUT,95) LOAD,IXBART,IYBART,AIXT,AYBART
ISN 0117       95 FORMAT ( 9X, 'LOAD = ', F10.4,' KIPS'//9X, 'MOMENT OF INERTIA ABOU
                 1T X CENTROIDAL AXIS = ',F10.4,' IN. TO THE FORTH'//9X,
                 2 'MOMENT OF INERTIA ABOUT Y CENTROIDAL AXIS = ',F10.4, ' IN. TO TH
                 3E FORTH'// 9X, ' AIXT = ',F10.4, ' SQUARE IN'//9X,'AYBART = ',
                 4F10.4,'CUBIC IN.')
            C
            C     COMPUTE COORDINATES OF NODE POINTS- XC(I),YC(I) - WITH RESPECT TO
            C     CENTROIDAL AXIS
            C
ISN 0118          L1 = L(1)
ISN 0119          L2 = L(2)
ISN 0120          L3 = L(3)
ISN 0121          D1 = D(1)
ISN 0122          D2 = D(2)
ISN 0123          D3 = D(3)
ISN 0124          T1 = T(1)
ISN 0125          T2 = T(2)
ISN 0126          T3 = T(3)
ISN 0127          D11 = D(1)
ISN 0128          D22 = D(2)
ISN 0129          D33 = D(3)
            C
            C     NODE POINTS - SECTION 1
```

```
                    C
ISN 0130                  DIV1 = D1 + 1
ISN 0131                  DO 150 I=1,DIV1
ISN 0132                  YC(I) = L2*COS(THETA) - YBAR
ISN 0133                  F = I
ISN 0134                  IF (I.EQ.1) GO TO 149
ISN 0136                  XC(I) = -(L1-(F-1.)*L1/D11)- L3 - L2*SIN(THETA)
ISN 0137                  GO TO 150
ISN 0138              149 XC(I) = -L1-L3-L2*SIN(THETA)
ISN 0139              150 CONTINUE
                    C
                    C     NODE POINTS - SECTION 2
                    C
ISN 0140                  DIV2A = DIV1 + 1
ISN 0141                  DIV2B = D1 + D2 + 1
ISN 0142                  DO 155 I=DIV2A,DIV2B
ISN 0143                  S=DIV1
ISN 0144                  TT = I
ISN 0145                  YC(I) = L2*COS(THETA) - ((TT-S)*L2/D22*COS(THETA)) - YBAR
ISN 0146                  XC(I) = -L3 - (L2*SIN(THETA)-L2/D22*(TT-S)*SIN(THETA))
ISN 0147              155 CONTINUE
                    C
                    C     NODE POINTS - SECTION 3
                    C
ISN 0148                  DIV3A = DIV2B + 1
ISN 0149                  DIV3B = D1 + D2 + D3 + 1
ISN 0150                  DO 160 I=DIV3A,DIV3B
ISN 0151                  S = DIV2B
ISN 0152                  TT = I
ISN 0153                  YC(I) = -YBAR
ISN 0154                  XC(I) = -(L3-(TT-S)*L3/D33)
ISN 0155              160 CONTINUE
                    C
                    C     REARRANGE INDICES AND DETERMINE NODE POINTS BY SYMMETRY FOR SECTIONS 4,5,6
                    C
ISN 0156                  JJ = D1 + D2 + D3
ISN 0157                  DO 165 J=1,JJ
ISN 0158                  I = 2*JJ + 1 - (J-1)
ISN 0159                  YC(I) = YC(J)
ISN 0160                  XC(I) = -XC(J)
ISN 0161              165 CONTINUE
                    C
                    C     COMPUTE ROE(I,J) FOR EACH ELEMENT
                    C
                    C     ROE(I,J) - SECTION 1
                    C
ISN 0162                  DO 170 I=1,D1
ISN 0163                  J = I + 1
ISN 0164                  ROE(I,J) = -(L2*COS(THETA)-YBAR)
ISN 0165              170 CONTINUE
                    C
                    C     ROE(I,J) - SECTION 2
                    C
ISN 0166                  ROE2= (L3+YBAR*TAN(THETA))*COS(THETA)
ISN 0167                  DD1 = D1 + 1
ISN 0168                  DDD2 = D1 + D2
ISN 0169                  DO 175 I=DD1,DDD2
```

```
ISN 0170          J = I + 1
ISN 0171          ROE(I,J) = ROE2
ISN 0172      175 CONTINUE
            C
            C     ROE(I,J) - SECTION 3
            C
ISN 0173          DD2 = DD1 + D2
ISN 0174          DDD3 = D1 + D2 + D3
ISN 0175          DO 180 I=DD2,DDD3
ISN 0176          J = I + 1
ISN 0177          ROE(I,J) = YBAR
ISN 0178      180 CONTINUE
            C
            C     REARRANGE INDICES AND DETERMINE ROE(I,J) BY SYMMETRY FOR SECTIONS 4,5,6
            C
ISN 0179          DO 185 K=1,DDD3
ISN 0180          KK = K + 1
ISN 0181          I = 2*DDD3 - (K-1)
ISN 0182          J = I + 1
ISN 0183          ROE(I,J) = ROE(K,KK)
ISN 0184      185 CONTINUE
            C
            C     REARRANGE INDICES SO THAT TOTAL STRAIN FACTOR,FF(I,J),APPLIES TO SEQUENCE
            C     OF NODE POINTS
            C
ISN 0185          DO 190 I=1,D1
ISN 0186          II = 1
ISN 0187          J = I + 1
ISN 0188          FF(I,J) = XQ(II,I)
ISN 0189      190 CONTINUE
ISN 0190          DO 195 IJ=1,D2
ISN 0191          II = 2
ISN 0192          I = IJ + D1
ISN 0193          J = I + 1
ISN 0194          FF(I,J) = XQ(II,IJ)
ISN 0195      195 CONTINUE
ISN 0196          DO 205 IJ=1,D3
ISN 0197          II = 3
ISN 0198          I = IJ + D1 + D2
ISN 0199          J = I + 1
ISN 0200          FF(I,J) = XQ(II,IJ)
ISN 0201      205 CONTINUE
ISN 0202          IK = D1 + D2 + D3
ISN 0203          DO 210 K=1,IK
ISN 0204          KK = K + 1
ISN 0205          I = 2*IK - (K-1)
ISN 0206          J = I + 1
ISN 0207          FF(I,J) = FF(K,KK)
ISN 0208      210 CONTINUE
ISN 0209          DD1 = D1 + 1
ISN 0210          DD2 = DD1 + D2
ISN 0211          DD3 = DD2 + D3
ISN 0212          DD4 = DD3 + D3
ISN 0213          DD5 = DD4 + D2
ISN 0214          DDD5 = 2*D1 + 2*D2 + 2*D3
ISN 0215          WRITE (OUTPUT,306)
ISN 0216      306 FORMAT ('1',9X,'I',15X,'J',15X,'W(J)'//)
```

```
ISN 0217          DO 240 I=1,DDD5
ISN 0218          J = I + 1
ISN 0219          W(1) = 0.0
ISN 0220          IF (J.GT.DD5) GO TO 235
ISN 0222          IF (J.GT.DD4) GO TO 230
ISN 0224          IF (J.GT.DD3) GO TO 225
ISN 0226          IF (J.GT.DD2) GO TO 220
ISN 0228          IF (J.GT.DD1) GO TO 215
              C
              C   COMPUTE VALUES OF W(J)
              C
ISN 0230          W(J) = W(I) +  ROE(I,J)*L1/D11
ISN 0231      307 FORMAT (9X,I5,10X,I5,10X,F10.4//)
ISN 0232          GO TO 240
ISN 0233      215 W(J) = W(I) +  ROE(I,J)*L2/D22
ISN 0234          GO TO 240
ISN 0235      220 W(J) = W(I) +  ROE(I,J)*L3/D33
ISN 0236          GO TO 240
ISN 0237      225 W(J) = W(I) +  ROE(I,J)*L3/D33
ISN 0238          GO TO 240
ISN 0239      230 W(J) = W(I) +  ROE(I,J)*L2/D22
ISN 0240          GO TO 240
ISN 0241      235 W(J) = W(I) +  ROE(I,J)*L1/D11
ISN 0242      240 CONTINUE
              C
              C   COMPUTE  IWX AND IWY
              C
ISN 0243          IWX = 0.00
ISN 0244          IWY = 0.00
ISN 0245          DO 270 I=1,DDD5
ISN 0246          J = I + 1
ISN 0247          IF (J.GT.DD5) GO TO 265
ISN 0249          IF (J.GT.DD4) GO TO 260
ISN 0251          IF (J.GT.DD3) GO TO 255
ISN 0253          IF (J.GT.DD2) GO TO 250
ISN 0255          IF (J.GT.DD1) GO TO 245
ISN 0257          IWX = IWX + 1./3.*(W(I)*XC(I)+W(J)*XC(J))*T1*L1/D11*FF(I,J)+ 1./6.
                 1*(W(I)*XC(J)+W(J)*XC(I))*T1*L1/D11*FF(I,J)
ISN 0258          IWY = IWY + 1./3.*(W(I)*YC(I)+W(J)*YC(J))*T1*L1/D11*FF(I,J)+ 1./6.
                 1*(W(I)*YC(J)+W(J)*YC(I))*T1*L1/D11*FF(I,J)
ISN 0259      309 FORMAT (9X,I5,9X,I5,10X,F10.4,8X,F10.4//)
ISN 0260          GO TO 270
ISN 0261      245 IWX = IWX + 1./3.*(W(I)*XC(I)+W(J)*XC(J))*T2*L2/D22*FF(I,J)+ 1./6.
                 1*(W(I)*XC(J)+W(J)*XC(I))*T2*L2/D22*FF(I,J)
ISN 0262          IWY = IWY + 1./3.*(W(I)*YC(I)+W(J)*YC(J))*T2*L2/D22*FF(I,J)+ 1./6.
                 1*(W(I)*YC(J)+W(J)*YC(I))*T2*L2/D22*FF(I,J)
ISN 0263          GO TO 270
ISN 0264      250 IWX = IWX + 1./3.*(W(I)*XC(I)+W(J)*XC(J))*T3*L3/D33*FF(I,J)+ 1./6.
                 1*(W(I)*XC(J)+W(J)*XC(I))*T3*L3/D33*FF(I,J)
ISN 0265          IWY = IWY + 1./3.*(W(I)*YC(I)+W(J)*YC(J))*T3*L3/D33*FF(I,J)+ 1./6.
                 1*(W(I)*YC(J)+W(J)*YC(I))*T3*L3/D33*FF(I,J)
ISN 0266          GO TO 270
ISN 0267      255 IWX = IWX + 1./3.*(W(I)*XC(I)+W(J)*XC(J))*T3*L3/D33*FF(I,J)+ 1./6.
                 1*(W(I)*XC(J)+W(J)*XC(I))*T3*L3/D33*FF(I,J)
ISN 0268          IWY = IWY + 1./3.*(W(I)*YC(I)+W(J)*YC(J))*T3*L3/D33*FF(I,J)+ 1./6.
                 1*(W(I)*YC(J)+W(J)*YC(I))*T3*L3/D33*FF(I,J)
ISN 0269          GO TO 270
```

```
ISN 0270      260 IWX = IWX + 1./3.*(W(I)*XC(I)+W(J)*XC(J))*T2*L2/D22*FF(I,J)+ 1./6.
                 1*(W(I)*XC(J)+W(J)*XC(I))*T2*L2/D22*FF(I,J)
ISN 0271          IWY = IWY + 1./3.*(W(I)*YC(I)+W(J)*YC(J))*T2*L2/D22*FF(I,J)+ 1./6.
                 1*(W(I)*YC(J)+W(J)*YC(I))*T2*L2/D22*FF(I,J)
ISN 0272          GO TO 270
ISN 0273      265 IWX = IWX + 1./3.*(W(I)*XC(I)+W(J)*XC(J))*T1*L1/D11*FF(I,J)+ 1./6.
                 1*(W(I)*XC(J)+W(J)*XC(I))*T1*L1/D11*FF(I,J)
ISN 0274          IWY = IWY + 1./3.*(W(I)*YC(I)+W(J)*YC(J))*T1*L1/D11*FF(I,J)+ 1./6.
                 1*(W(I)*YC(J)+W(J)*YC(I))*T1*L1/D11*FF(I,J)
ISN 0275      270 CONTINUE
              C
              C       COMPUTE COORDINATES OF SHEAR CENTRE (WITH CENTROID AS REFERENCE)
              C
ISN 0276          XO = IWY/IXBART
ISN 0277          YO = -IWX/IYBART
ISN 0278          WRITE (OUTPUT,275) XO,YO
ISN 0279      275 FORMAT ('1',9X,'X COORDINATE OF SHEAR CENTER (WRT CENTROID) = ',F1
                 10.4,' IN.'//9X,'Y COORDINATE OF SHEAR CENTER (WRT CENTROID) = ',F1
                 20.4,' IN.')
              C       COMPUTE ROEO(I,J) ABOUT SHEAR CENTRE
              C
              C       CHECK ON RELATIVE POSITION OF SHEAR CENTRE IN ORDER TO DETERMINE SIGN OF
              C       ROEO
              C
ISN 0280          DD2 = D1 + D2 + 1
ISN 0281          DD1 = D1 + 1
ISN 0282          YY2 = L(2)*COS(THETA)-YBAR+ABS(YO)
ISN 0283          BETA = ATAN((L2*SIN(THETA)+L3)/YY2)
ISN 0284          IF (BETA.GT.THETA) GO TO 305
ISN 0286          SIGN = -1.000
ISN 0287          GO TO 310
ISN 0288      305 SIGN = 1.000
ISN 0289      310 THBET = ABS(THETA-BETA)
ISN 0290          ROE2 = SIN(THBET)*(ABS(YO)-YBAR+L(2)*COS(THETA))/COS(BETA)
ISN 0291          DO 335 I=1,DDD5
ISN 0292          J = I + 1
ISN 0293          IF (J.GT.DD5) GO TO 330
ISN 0295          IF (J.GT.DD4) GO TO 325
ISN 0297          IF (J.GT.DD2) GO TO 320
ISN 0299          IF (J.GT.DD1) GO TO 315
ISN 0301          ROEO(I,J) = -(ABS(YO)+L2*COS(THETA)-YBAR)
ISN 0302          GO TO 335
ISN 0303      315 ROEO(I,J) = ROE2*SIGN
ISN 0304          GO TO 335
ISN 0305      320 ROEO(I,J) = -(ABS(YO) - YBAR)
ISN 0306          GO TO 335
ISN 0307      325 ROEO(I,J) = ROE2*SIGN
ISN 0308          GO TO 335
ISN 0309      330 ROEO(I,J) = -(ABS(YO)+L(2)*COS(THETA)-YBAR)
ISN 0310      335 CONTINUE
              C       COMPUTE WO(J)
ISN 0311          WO(1) = 0.00
ISN 0312          AREA  = 0.00
ISN 0313      323 FORMAT (9X,I5,10X,I5,10X,F10.4,10X,F10.4//)
ISN 0314          DO 365 I=1,DDD5
ISN 0315          J = I + 1
ISN 0316          IF (J.GT.DD5) GO TO 360
```

```
ISN 0318          IF (J.GT.DD4) GO TO 355
ISN 0320          IF (J.GT.DD3) GO TO 350
ISN 0322          IF (J.GT.DD2) GO TO 345
ISN 0324          IF (J.GT.DD1) GO TO 360
ISN 0326          WO(J) = WO(I) + ROEO(I,J)*L1/D11
ISN 0327          AREA = AREA + L1/D11*FF(I,J)*T1
ISN 0328          GO TO 365
ISN 0329      340 WO(J) = WO(I) + ROEO(I,J)*L2/D22
ISN 0330          AREA = AREA + L2/D22*FF(I,J)*T2
ISN 0331          GO TO 365
ISN 0332      345 WO(J) = WO(I) + ROEO(I,J)*L3/D33
ISN 0333          AREA = AREA + L3/D33*FF(I,J)*T3
ISN 0334          GO TO 365
ISN 0335      350 WO(J) = WO(I) + ROEO(I,J)*L3/D33
ISN 0336          ARFA = AREA + L3/D33*FF(I,J)*T3
ISN 0337          GO TO 365
ISN 0338      355 WO(J) = WC(I) + ROEO(I,J)*L2/D22
ISN 0339          AREA = AREA + L2/D22*FF(I,J)*T2
ISN 0340          GO TO 365
ISN 0341      360 WO(J) = WO(I) + ROEO(I,J)*L1/D11
ISN 0342          AREA = AREA + L1/D11*FF(I,J)*T1
ISN 0343      365 CONTINUE
            C
            C     COMPUTE WN(J)
            C
ISN 0344          WWN = 0.00
ISN 0345          DO 395 I=1,DDD5
ISN 0346          J = I + 1
ISN 0347          IF (J.GT.DD5) GO TO 390
ISN 0349          IF (J.GT.DD4) GO TO 385
ISN 0351          IF (J.GT.DD3) GO TO 380
ISN 0353          IF (J.GT.DD2) GO TO 375
ISN 0355          IF (J.GT.DD1) GO TO 370
ISN 0357          WWN = (WO(I)+WO(J))*T1*L1/D11*FF(I,J) + WWN
ISN 0358          GO TO 395
ISN 0359      370 WWN = WWN + (WO(I)+WO(J))*T2*L2/D22*FF(I,J)
ISN 0360          GO TO 395
ISN 0361      375 WWN = WWN + (WO(I)+WO(J))*T3*L3/D33*FF(I,J)
ISN 0362          GO TO 395
ISN 0363      380 WWN = WWN + (WO(I)+WO(J))*T3*L3/D33*FF(I,J)
ISN 0364          GO TO 395
ISN 0365      385 WWN = WWN + (WO(I)+WO(J))*T2*L2/D22*FF(I,J)
ISN 0366          GO TO 395
ISN 0367      390 WWN = WWN + (WO(I)+WO(J))*T1*L1/D11*FF(I,J)
ISN 0368      395 CONTINUE
ISN 0369      324 FORMAT ('1',9X,'WWN = ',F10.4//)
ISN 0370      327 FORMAT (9X,I5,9X,F10.4//)
ISN 0371          KK = DDD5 + 1
ISN 0372          DO 405 I=1,KK
ISN 0373          WN(I) = WWN/(2.0*AREA) - WO(I)
ISN 0374      405 CONTINUE
            C
            C     COMPUTE IW AND KT
            C
ISN 0375          IW = 0.0
ISN 0376          KT = 0.0
ISN 0377          DO 435 I=1,DDD5
```

```
ISN 0378          J = I + 1
ISN 0379          IF (J.GT.DD5) GO TO 430
ISN 0381          IF (J.GT.DD4) GO TO 425
ISN 0383          IF (J.GT.DD3) GO TO 420
ISN 0385          IF (J.GT.DD2) GO TO 415
ISN 0387          IF (J.GT.DD1) GO TO 410
ISN 0389          IW = IW + 1./3.*(WN(I)*WN(I)+WN(I)*WN(J)+WN(J)*WN(J))*T1*L1/D11*FF
                 1(I,J)
ISN 0390          KT = KT + 1./3.*((T1**3)*L1/D11)
ISN 0391      329 FORMAT (9X,I5,4X,I5,12X,F10.4,9X,F10.4//)
ISN 0392          GO TO 435
ISN 0393      410 IW = IW + 1./3.*(WN(I)*WN(I)+WN(I)*WN(J)+WN(J)*WN(J))*T2*L2/D22*FF
                 1(I,J)
ISN 0394          KT = KT + 1./3.*((T2**3)*L2/D22)
ISN 0395          GO TO 435
ISN 0396      415 IW = IW + 1./3.*(WN(I)*WN(I)+WN(I)*WN(J)+WN(J)*WN(J))*T3*L3/D33*FF
                 1(I,J)
ISN 0397          KT = KT + 1./3.*((T3**3)*L3/D33)
ISN 0398          GO TO 435
ISN 0399      420 IW = IW + 1./3.*(WN(I)*WN(I)+WN(I)*WN(J)+WN(J)*WN(J))*T3*L3/D33*FF
                 1(I,J)
ISN 0400          KT = KT + 1./3.*((T3**3)*L3/D33)
ISN 0401          GO TO 435
ISN 0402      425 IW = IW + 1./3.*(WN(I)*WN(I)+WN(I)*WN(J)+WN(J)*WN(J))*T2*L2/D22*FF
                 1(I,J)
ISN 0403          KT = KT + 1./3.*((T2**3)*L2/D22)
ISN 0404          GO TO 435
ISN 0405      430 IW = IW + 1./3.*(WN(I)*WN(I)+WN(I)*WN(J)+WN(J)*WN(J))*T1*L1/D11*FF
                 1(I,J)
ISN 0406          KT = KT + 1./3.*((T1**3)*L1/D11)
ISN 0407      435 CONTINUE
ISN 0408          WRITE (OUTPUT,331)IXBART,IYBART,XO,YO,IW,KT
ISN 0409      331 FORMAT ('1',9X,'IX = ',F10.4,' IN. TO THE FORTH'//9X,'IY = ',F10.4
                 1,' IN. TO THE FORTH'//9X,'XO = ',F10.4,' IN.'//9X,'YO = ',F10.4,'
                 2IN.'//9X'IW = ',F10.4//9X,'KT = ',F10.4//)
               C          COMPUTE KBAR
ISN 0410          BARK=0.0
ISN 0411          DO 1201 I=1,3
ISN 0412          P=D(I)
ISN 0413          DUM1=T(I)*L(I)/P
ISN 0414          DO 1202 K=1,P
               C          ST(I,K)=STRAIN IN SECTION I DIV K COMPUTED PRIOR
ISN 0415          IF(ST(I,K).LT.SY(I,K))GO TO 1203
ISN 0417          IF(ST(I,K).GT.SS(I,K))GO TO 1204
ISN 0419          TRES=STRESY(I,K)
ISN 0420          GO TO 1205
ISN 0421     1204 TRES=STRESY(I,K)+(ST(I,K)-SS(I,K))*ES
ISN 0422          GO TO 1205
ISN 0423     1203 TRES=E*ST(I,K)
ISN 0424     1205 CONTINUE
               C          COMPUTE COORDS OF CENTRE OF ELEMENT
ISN 0425          IF(I.EQ.2)GO TO 1206
ISN 0427          IF(I.EQ.3)GO TO 1207
ISN 0429          IIN=K
ISN 0430          JJN=K+1
ISN 0431          GO TO 1208
ISN 0432     1206 IIN=K+D(1)
```

```
ISN 0433            JJN=IIN+1
ISN 0434            GO TO 1208
ISN 0435      1207  IIN=K+D(1)+D(2)
ISN 0436            JJN=IIN+1
ISN 0437      1208  CONTINUE
ISN 0438            XXEL=(XC(IIN)+XC(JJN))/2.
ISN 0439            YYEL=(YC(IIN)+YC(JJN))/2.
ISN 0440            AAAAK=(XXEL-XO)*(XXEL-XO)+(YYEL-YO)*(YYEL-YO)
ISN 0441            BARK=(2.*AAAAK*TRES*DUM1)*(-1.)+BARK
ISN 0442      1202  CONTINUE
ISN 0443      1201  CONTINUE
                 C      PROGRAM LCRIT,COMPUTES CRIT LENGTH FOR DIFFERENT BUCKLING MODES
ISN 0444            WRITE(6,501)
ISN 0445       501  FORMAT(1H1,20X,'CRITICAL LENGTHS ARE AS BELOW'////)
ISN 0446            IF(SSS.EQ.100.) GO TO 1000
                 C      PRINT OUT TITLE AND THEN ECHO CHECK DATA
ISN 0448            WRITE (6,502)SSS,LOAD
ISN 0449       502  FORMAT(1H ,'CRIT.LENGTHS FOR SECTION'F3.1,4H     ,'AXIAL LOAD='F6.1
                   1)
ISN 0450            WRITE (6,503) IXBART,IYBART,IW,KT,AREA,E,G,YO
ISN 0451       503  FORMAT(1HO,'SECT.PROPS.IX='F7.2,' IY='F7.2,' IW='F7.2,' KT=' F7.2,
                   1' A='F8.2,' E='F8.1,' G='F8.1,' YO='F5.2)
                 C      COMPUTE CRIT LENGTH CORREOSPONDING TO BUCKLING ABT  XX AXIS
ISN 0452            PIE=3.14159
ISN 0453            LX=SQRT((PIE*PIE*E*IXBART)/LOAD)
ISN 0454            WRITE(6,505)LX
ISN 0455       505  FORMAT(1H ,10X,'CRIT.LENGTH W.R. TO X/X AXIS BUCKLE='F7.2)
                 C      SOLVE CRIT LENGTH LAT.TORSIONAL BUCKLE
ISN 0456            AZ=PIE*PIE*E*IYBART
ISN 0457            BZ=G*KT
ISN 0458            CZ=PIE*PIE*E*IW
ISN 0459            DZ=LOAD*YO*LOAD*YO
ISN 0460            AAZ=LOAD*BZ+LOAD*BARK+DZ
ISN 0461            BBZ=LOAD*CZ-AZ*BARK-AZ*BZ
ISN 0462            CC=-1.*(AZ*CZ)
ISN 0463            ZAZ=BBZ*BBZ-4.*AAZ*CC
ISN 0464            IF(ZAZ.LT.0.)GO TO 1301
ISN 0466            ZZAZ=(-BBZ+SQRT(ZAZ))/(2.*AAZ)
ISN 0467            IF(ZZAZ.LT.0.)GO TO 1301
ISN 0469            AL=SQRT((-BBZ+SQRT(BBZ*BBZ-4.*AAZ*CC))/(2.*AAZ))
ISN 0470            GO TO 1302
ISN 0471      1301  AL=0.0
ISN 0472      1302  CONTINUE
ISN 0473            IF(ZAZ.LT.0.)GO TO 1303
ISN 0475            BZAZ=(-BBZ-SQRT(ZAZ))/(2.*AAZ)
ISN 0476            IF(BZAZ.LT.0.)GO TO 1303
ISN 0478            BL=SQRT((-BBZ-SQRT(BBZ*BBZ-4.*AAZ*CC))/(2.*AAZ))
ISN 0479            GO TO 507
ISN 0480      1303  BL=0.
ISN 0481       507  WRITE(6,504)AL,BL
ISN 0482       504  FORMAT(1HO,'CRIT.LENGTH W.R.TO LAT/TORS.BUCKLE='F7.2,'INS OR'F7.2,
                   1'INS')
                 C      PROGRAM COMPUTES CRITICAL LENGTHS FOR DIFFERENT BUCKLING MODES
                 C      SECOND PART COMPUTES ALLOWABLE AXIAL LOAD THAT CAN BE CARRIED ON
                 C      SECTION W.R. CODE PROVISIONS
                 C      SECOND PART-DATA COMPUTED IN FIRST PART
ISN 0483            FY=55.
```

```
ISN 0484          JSS=SSS
ISN 0485          IF(JSS-2)520,530,540
            C     IF(JSS-2)IS -VE ,SECTION E ;ZERO,SECTION F;TVE,SECTION L
ISN 0486      520 CONTINUE
ISN 0487          AA=3.105
ISN 0488          RXX=.877
ISN 0489          GO TO 550
ISN 0490      530 RXX=0.898
ISN 0491          AA=3.795
ISN 0492          GO TO 550
ISN 0493      540 RXX=0.446
ISN 0494          AA=2.237
ISN 0495          GO TO 550
            C     VALUES OF CO,CP,M GIVEN IN 1970 CODE FOR FY=55KSI
ISN 0496      550 CO=19.
ISN 0497          CP=82.5
ISN 0498          ZM=0.175
            C     SIMP.SUPP. K=1 HAVE 3 POSS CRIT.LENGTHSAL,BL,LX
            C     IF BL.EQ.0,BL IS NOT APPLICABLE
ISN 0499          LL(3)=BL
ISN 0500          LL(2)=AL
ISN 0501          LL(1)=LX
ISN 0502          IF(BL.EQ.0.)GO TO 551
ISN 0504          NN=3
ISN 0505          GO TO 552
ISN 0506      551 NN=2
ISN 0507      552 DO 553 JJ=1,NN
ISN 0508          KLR=LL(JJ)/RXX
ISN 0509          IF(KLR.GT.CO)GO TO 570
ISN 0511          FA=0.6*55.
ISN 0512          PP=AA*FA
ISN 0513          GO TO 580
ISN 0514      570 IF(KLR.GT.CP)GO TO 590
ISN 0516          FA=0.60*FY-ZM*(KLR-CO)
ISN 0517          PP=AA*FA
ISN 0518          GO TO 580
ISN 0519      590 FA=149000./(KLR*KLR)
ISN 0520          PP=AA*FA
ISN 0521      580 LLL=LL(JJ)
ISN 0522          WRITE(6,600)LLL,PP
ISN 0523      600 FORMAT(///10X,'EFFECTIVE LENGTH='F6.1,4H     ,/10X,'CRIT LOAD BY CO
                 1DE='F6.1)
ISN 0524      553 CONTINUE
ISN 0525          GO TO 3
ISN 0526      999 CALL EXIT
ISN 0527     1000 STOP
ISN 0528          END

COMPILATION DELETED. 1
```